AGU PUBLICATIONS

JGR

Journal of Geophysical Research: Solid Earth

RESEARCH ARTICLE
10.1002/2017JB014308

**Key Points:**
- Newly identified marine magnetic anomalies document the formation and evolution of the ENAM and western North Atlantic Ocean
- Early Atlantic seafloor spreading rates and ridge orientations indicate possible asymmetric crustal accretion
- Early seafloor spreading may have been influenced by preexisting margin structure and may have included short lived propagating rifts

**Supporting Information:**
- Supporting Information S1
- Data Set S1

**Correspondence to:**
J. A. Greene,
greene@tamu.edu

**Citation:**
Greene, J. A., Tominaga, M., Miller, N. C., Hutchinson, D. R., & Karl, M. R. (2017). Refining the formation and early evolution of the Eastern North American Margin: New insights from multiscale magnetic anomaly analyses. *Journal of Geophysical Research: Solid Earth*, *122*, 8724–8748. https://doi.org/10.1002/2017JB014308

Received 12 APR 2017
Accepted 11 OCT 2017
Accepted article online 17 OCT 2017
Published online 16 NOV 2017



# Refining the Formation and Early Evolution of the Eastern North American Margin: New Insights From Multiscale Magnetic Anomaly Analyses

**John A. Greene[1], Masako Tominaga[1], Nathaniel C. Miller[2], Deborah R. Hutchinson[2], and Matthew R. Karl[3]**

[1]Department of Geology and Geophysics, Texas A&M University, College Station, TX, USA, [2]U. S. Geological Survey, Woods Hole Coastal and Marine Science Center, Woods Hole, MA, USA, [3]Department of Earth and Environmental Sciences, Michigan State University, East Lansing, MI, USA

**Abstract** To investigate the oceanic lithosphere formation and early seafloor spreading history of the North Atlantic Ocean, we examine multiscale magnetic anomaly data from the Jurassic/Early Cretaceous age Eastern North American Margin (ENAM) between 31 and 40°N. We integrate newly acquired sea surface magnetic anomaly and seismic reflection data with publicly available aeromagnetic and composite magnetic anomaly grids, satellite-derived gravity anomaly, and satellite-derived and shipboard bathymetry data. We evaluate these data sets to (1) refine magnetic anomaly correlations throughout the ENAM and assign updated ages and chron numbers to M0–M25 and eight pre-M25 anomalies; (2) identify five correlatable magnetic anomalies between the East Coast Magnetic Anomaly (ECMA) and Blake Spur Magnetic Anomaly (BSMA), which may document the earliest Atlantic seafloor spreading or synrift magmatism; (3) suggest preexisting margin structure and rifting segmentation may have influenced the seafloor spreading regimes in the Atlantic Jurassic Quiet Zone (JQZ); (4) suggest that, if the BSMA source is oceanic crust, the BSMA may be M series magnetic anomaly M42 (~168.5 Ma); (5) examine the along and across margin variation in seafloor spreading rates and spreading center orientations from the BSMA to M25, suggesting asymmetric crustal accretion accommodated the straightening of the ridge from the bend in the ECMA to the more linear M25; and (6) observe anomalously high-amplitude magnetic anomalies near the Hudson Fan, which may be related to a short-lived propagating rift segment that could have helped accommodate the crustal alignment during the early Atlantic opening.

## 1. Introduction

The Eastern North American Margin (ENAM) (Figure 1) was formed by the opening of the North Atlantic Ocean following the rifting of the last supercontinent, Pangaea (Wilson, 1966). Advancing knowledge on the structure and development of the ENAM is critical for understanding not only the formation and evolution of passive margins (Sheridan, 1989; Withjack et al., 1998) but also the early opening history of the Atlantic Ocean (Biari et al., 2017; Bird et al., 2007; Klitgord & Schouten, 1986; Kneller et al., 2012; Labails et al., 2010; Schettino & Turco, 2009; Vogt, 1973). Furthermore, the rift-drift transition of the ENAM was coincident with and may have been triggered by the volcanism of the Central Atlantic Magmatic Province (Marzoli et al., 1999; Olsen et al., 2003; Schlische et al., 2003), which is also thought to be associated with a mass extinction event at the Triassic-Jurassic boundary (Nomade et al., 2007). Additionally, the architecture of the ENAM influences the prevalence and distribution of geohazards, including earthquakes and submarine landslides (Chapman & Beale, 2010; Chaytor et al., 2007; Embley & Jacobi, 1986; Folger, 1988), and the origin and extent of natural resources (Dillon et al., 1986; Mattick & Libby-French, 1986; Riggs & Manheim, 1988).

M series (Mesozoic) magnetic anomalies have been critical in characterizing the formation history of the ENAM. Many studies have identified M series magnetic anomalies in the ENAM and western North Atlantic from M0 to M25, suggesting a slow spreading regime and an absence of ridge jumps (e.g., Bird et al., 2007; Klitgord & Schouten, 1986; Labails et al., 2010; Müller et al., 1997; Schettino & Turco, 2009; Sundvik & Larson, 1988; Tominaga & Sager, 2010a, 2010b; Vogt, 1986). For the earlier stage of the ENAM formation, however, only a few studies could extend magnetic anomaly identifications beyond anomaly M25 into the Atlantic Jurassic Quiet Zone (JQZ) (Barrett & Keen, 1976; Bird et al., 2007) due to the low-amplitude magnetic anomalies that cause difficulty in identification (Figure 1a) (Bird et al., 2007; Larson & Pitman, 1972; Vogt,

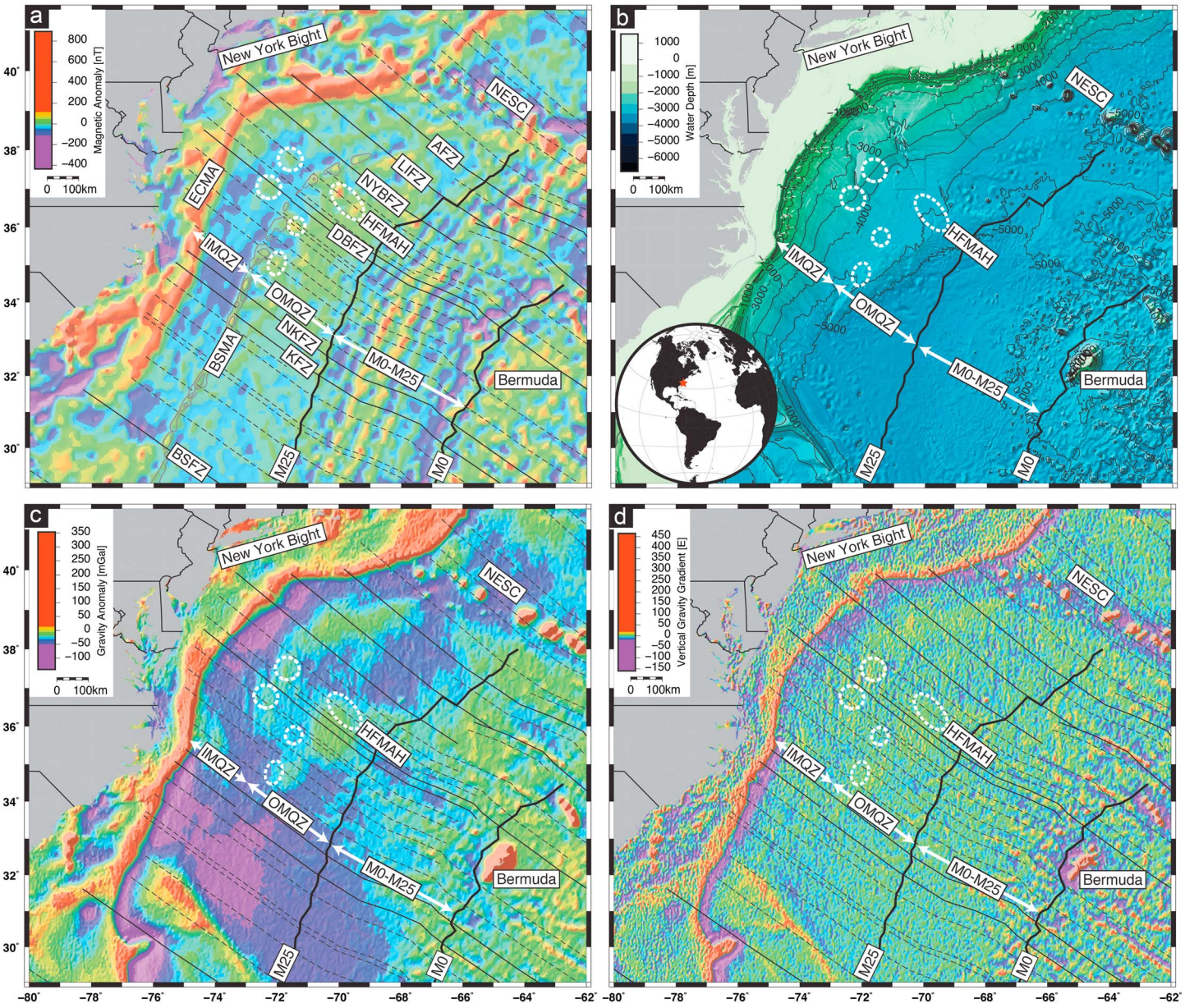


**Figure 1.** Geophysical data for the ENAM: (a) EMAG2v3 composite magnetic anomaly grid (Meyer et al., 2016), (b) ETOPO1 satellite-derived bathymetry grid (Amante & Eakins, 2009) contoured every 500 m, (c) satellite-derived gravity anomaly grid (Sandwell et al., 2014), and (d) satellite-derived vertical gravity gradient grid (Sandwell et al., 2014). Prominent features labeled: New York Bight, East Coast Magnetic Anomaly (ECMA), Blake Spur Magnetic Anomaly (BSMA), New England Seamount Chain (NESC), and island of Bermuda. White arrows show extent of the Inner Magnetic Quiet Zone (IMQZ) and Outer Magnetic Quiet Zone (OMQZ) subdivisions of the Atlantic JQZ, and M0–M25. White dashed circles indicate anomalous magnetic features, including the Hudson Fan Magnetic Anomaly High (HFMAH). Thick black lines indicate M series magnetic anomaly lineations M0 and M25. Dashed black lines are fracture zone picks of Klitgord and Schouten (1986). Solid black lines denote fracture zones referenced in this study: Blake Spur (BSFZ), Kane (KFZ), Northern Kane (NKFZ), Delaware Bay (DBFZ), New York Bight (NYBFZ), Long Island (LIFZ), and Atlantis (AFZ) (Klitgord & Schouten, 1986). Thin gray contours indicate BSMA (Klitgord & Schouten, 1986).

1986; Vogt et al., 1970). Furthermore, a notable change in magnetic anomaly strike is present from the significant bend in the East Coast Magnetic Anomaly (ECMA) offshore the New York Bight to the more linear M25 (Figure 1a) (Klitgord & Schouten, 1986); however, the origin of the apparent straightening has yet to be explained. Additionally, early along and across margin seafloor spreading rates and patterns during the formation of the Atlantic JQZ have not been comprehensively examined, despite the seafloor formation between rifting and the more thoroughly studied M0–M25 region being a significant piece of the early Atlantic opening history.

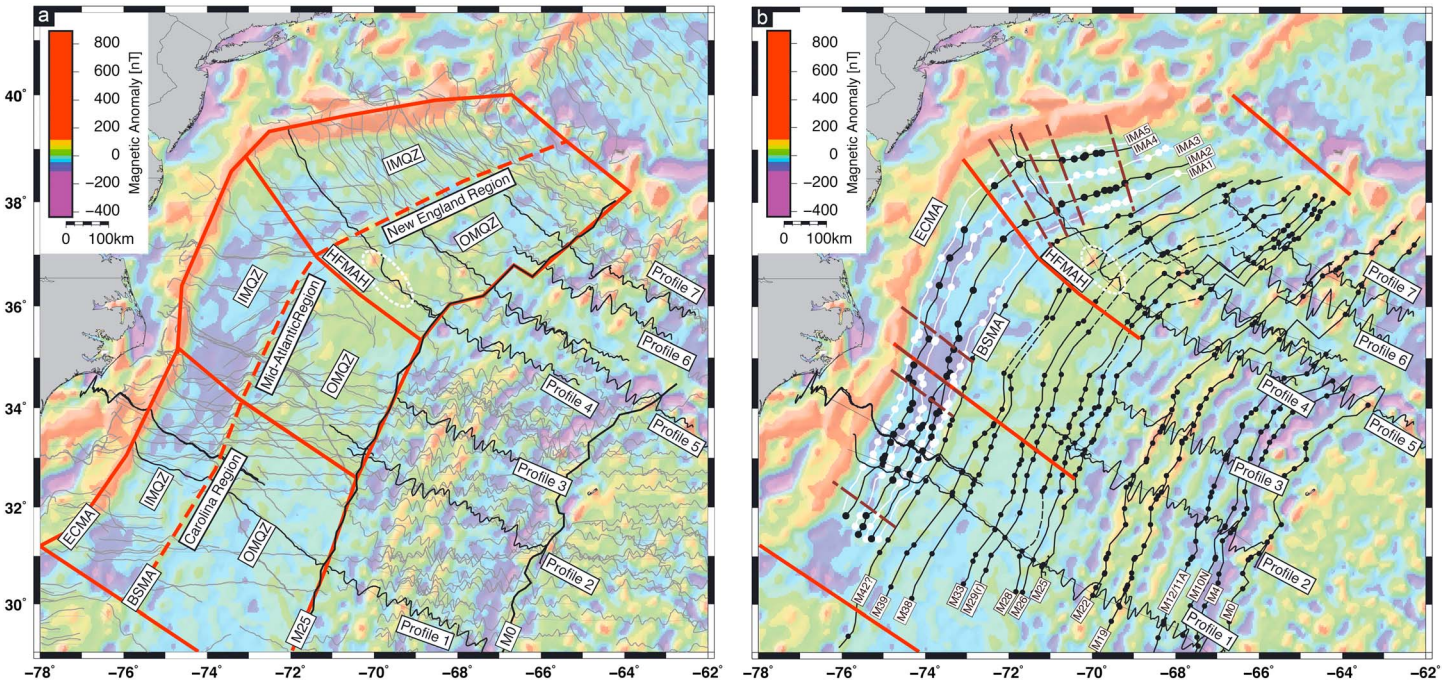


**Figure 2.** (a) EMAG2v3 composite magnetic anomaly grid (Meyer et al., 2016) with recently collected (Arsenault et al., 2017) and archived shipboard magnetic anomaly profiles from the NCEI overlain in gray. Red lines outline IMQZ and OMQZ of the New England, Mid-Atlantic, and Carolina regions. Black lines indicate M series magnetic anomaly lineations M0 and M25. Select profiles used in age/chron assignment and spreading rate calculations shown in black. Profiles 1, 2, 4, 5, and 7 consist of multiple segments concatenated together (see Figure 4). (b) EMAG2v3 composite magnetic anomaly grid (Meyer et al., 2016) with magnetic anomaly correlations overlain. Solid black lines show select M series magnetic anomaly lineations, with dashed sections denoting areas where there was difficulty tracing the lineations using the EMAG2v3 grid. Dots indicate location of corresponding magnetic anomalies on sea surface magnetic anomaly profiles. In IMQZ, solid lines indicate interpreted magnetic anomalies IMA1–IMA5 (black—peaks; white—troughs). Red lines denote boundaries of the New England, Mid-Atlantic, and Carolina regions. Dashed brown lines mark interpreted offsets in IMQZ magnetic anomalies IMA1–IMA5.

The prerift history of the eastern margin of the North American continent is likely to be an influence on the amount of volcanic activity experienced during continental breakup (Keen & Potter, 1995a) and the localization of rifting near the modern continental shelf (Dunbar & Sawyer, 1989; Manspeizer, 1988; Sheridan et al., 1993). The eastern edge of the North American Continent has experienced several cycles of tectonic collision and rifting throughout its formation history (e.g., Manspeizer, 1988; Wilson, 1966), resulting in a complex crustal structure from the accretion of terranes over time (Hatcher, 1989; Hatcher, 2010; Horton et al., 1989). However, the influence of preexisting structure on the subsequent seafloor spreading of the early Atlantic opening (e.g., Behn & Lin, 2000; Sawyer, 1985), particularly within the low-amplitude magnetic anomaly region of the Atlantic JQZ, has not been extensively investigated.

In this study, we examine the magnetic anomalies of the ENAM and western Atlantic to refine our understanding of the early Atlantic seafloor spreading regimes and influence of preexisting margin structure. We use recently collected (Arsenault et al., 2017) and archived sea surface magnetic data from the National Centers for Environmental Information (NCEI) (www.ncei.noaa.gov), aeromagnetic (Bankey et al., 2002; Zietz, 1982), and the newly available high-quality EMAG2v3 (version 3) global magnetic anomaly grid compiling satellite, aeromagnetic, and shipboard magnetic data (Meyer et al., 2016). We integrate these data with newly acquired multichannel seismic (MCS) data (Arsenault et al., 2017), and satellite-derived gravity (Sandwell et al., 2014) and bathymetry grids (Amante & Eakins, 2009; Andrews et al., 2016; Butman et al., 2006) (Figures 1 and 2). Based on magnetic anomaly analyses, we estimate seafloor spreading rates and patterns in the Outer Magnetic Quiet Zone (OMQZ) of the Atlantic JQZ between the Blake Spur Magnetic Anomaly (BSMA) and M25 (Figure 1a) (Klitgord & Grow, 1980) and from M0 to M25, revealing, for the first time, a more comprehensive view on the pre-M25 stage of seafloor spreading. We also identify correlatable magnetic anomalies in the Inner Magnetic Quiet Zone (IMQZ) of the Atlantic JQZ between the ECMA and BSMA (Figure 1a) (Klitgord & Grow, 1980) that have *not* previously been identified or discussed. We

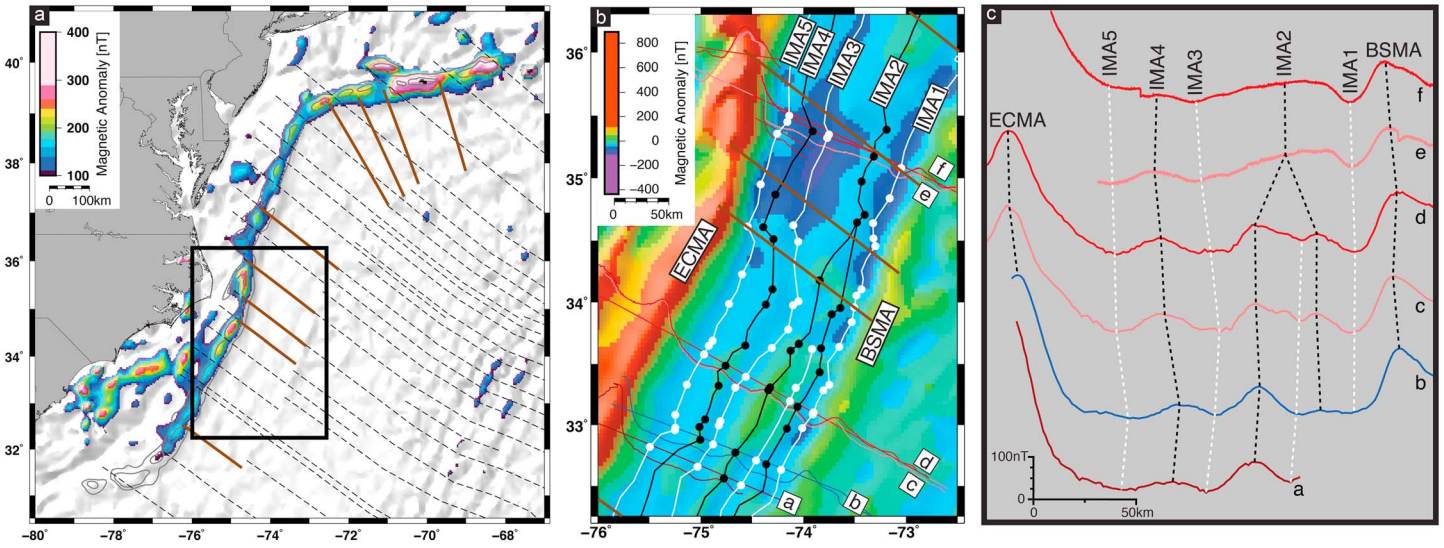


**Figure 3.** (a) EMAG2v3 composite magnetic anomaly grid (Meyer et al., 2016) with scale altered to highlight range of ECMA. ECMA contours in light gray showing segmentation (Klitgord & Schouten, 1986). Dashed black lines are fracture zone picks of Klitgord and Schouten (1986). Brown lines mark interpreted offsets in IMQZ magnetic anomalies IMA1–IMA5. Black box shows location of Figure 3b. (b) Close up of the IMQZ of the Carolina region (see Figure 3a for location). Overlays are recently collected (Arsenault et al., 2017) and archived shipboard magnetic anomaly profiles from the NCEI. Solid lines show interpreted magnetic anomalies IMA1–IM5 (black—peaks; white—troughs). Dots indicate location of corresponding magnetic anomalies on sea surface magnetic anomaly profiles (Figure 2a). Brown lines mark interpreted offsets in IMQZ magnetic anomalies IMA1–IMA5. Profiles b, c, and d make up Profile 1 (Figure 2). (c) Correlation of magnetic anomalies IMA1–IMA5 on select profiles within the IMQZ of the Carolina region. Dashed lines show magnetic anomaly correlations (black—peaks; white—troughs). ECMA and BSMA labeled. Magnetic anomaly profiles a–f correspond to profiles in Figure 3b.

provide our georeferenced, digital magnetic anomaly data to the wider community for use in future studies (Data Set S1 in the supporting information).

## 2. Background

### 2.1. ENAM Marine Magnetic Anomalies

Marine magnetic anomalies in the ENAM and western North Atlantic basin are one of the key observational data sets for understanding the formation and evolution of oceanic lithosphere during the Atlantic opening (Figures 1a and 2). Deciphering magnetic anomaly character provides insight into the tectonic framework of the ENAM, including prominent features like the ECMA and BSMA, the low-amplitude magnetic anomaly region of the Atlantic JQZ, and the M series magnetic anomalies M0–M25 (Figures 1a and 2).

The ECMA is a high-amplitude, positive magnetic anomaly that follows the margin for 2,500 km, near the edge of the continental shelf, from offshore Georgia (at the Blake Spur Fracture Zone) to Nova Scotia (Figure 1a) (Keen & Potter, 1995b; Keller et al., 1954; Klitgord & Schouten, 1986). The ECMA displays segmentation along its length, represented by a series of magnetic anomaly highs separated by zones of relatively lower amplitude (Figure 3a) (Behn & Lin, 2000; Klitgord & Schouten, 1986; Wyer & Watts, 2006). The ECMA has been thought to represent the continent ocean transition (Austin et al., 1990; Klitgord et al., 1988; Tréhu et al., 1989) and has been attributed to a late Paleozoic Alleghanian suture (McBride & Nelson, 1988) or seaward dipping reflectors (SDRs) formed by the emplacement and subsidence of volcanic layers during continental breakup (Austin et al., 1990; Benson, 2003; Keen & Potter, 1995b; Lizarralde & Holbrook, 1997; Oh et al., 1995; Talwani et al., 1995; Talwani & Abreu, 2000). Various ages have been proposed for the ECMA, with Klitgord and Schouten (1986) extrapolating an age of 175 Ma, while Benson (2003) suggested an updated age based on more recent geomagnetic timescales of 172 Ma to 179 Ma. A possible conjugate to the ECMA, the lower amplitude West African Coast Magnetic Anomaly, exists on the northwest African margin (Klitgord & Schouten, 1986; Labails et al., 2010; Sahabi et al., 2004).

The BSMA is another high-amplitude, positive magnetic anomaly in the Atlantic JQZ located 150–250 km to the east and oriented parallel to the ECMA, diminishing around 39°N (Figure 1a) (Klitgord & Schouten, 1986; Taylor et al., 1968; Vogt et al., 1970). The origin of this magnetic anomaly is unknown, but is thought to play a

key role in the early Atlantic opening (Bird et al., 2007; Klitgord & Schouten, 1986; Kneller et al., 2012; Labails et al., 2010; Schettino & Turco, 2009; Vogt, 1973). Like the ECMA, the BSMA is segmented along its length (Figure 1a) (Klitgord et al., 1988). Klitgord and Schouten (1986) extrapolated an age of 170 Ma for the BSMA, while Benson (2003) suggested an updated age based on more recent geomagnetic timescales of 168 Ma to 171 Ma. A possible conjugate to the BSMA, the African Blake Spur Magnetic Anomaly, has been proposed for the northwest African margin (Labails et al., 2010; Sahabi et al., 2004).

The Atlantic JQZ is a zone of low-amplitude magnetic anomalies between the ECMA and M25 (Figure 1a) (Larson & Pitman, 1972; Vogt, 1986; Vogt et al., 1970). The low magnetic anomaly amplitudes of the Atlantic JQZ have been attributed to a low intensity geomagnetic field rapidly reversing polarity and/or a low paleomagnetic latitude for the plate at the time of crustal formation (Larson & Pitman, 1972; Tivey et al., 2006; Tominaga & Sager, 2010a). The Atlantic JQZ can further be subdivided into two zones of low-amplitude magnetic anomalies: the IMQZ and OMQZ (Figure 1a) (Klitgord & Grow, 1980). The IMQZ of the Atlantic JQZ is an approximately 100 km wide (west to east) zone between the ECMA and BSMA (Figures 1a and 3b) (Klitgord & Grow, 1980; Vogt et al., 1971). Ages for the crust in the IMQZ are inferred to be older than 170 Ma, possibly as old as 190 Ma (Barrett & Keen, 1976; Bird et al., 2007; Klitgord & Schouten, 1986; Labails et al., 2010; Schettino & Turco, 2009; Sheridan, 1987; Vogt, 1973; Vogt, 1986). Furthermore, while the nature of the IMQZ crust is still unknown, Bird et al. (2007) proposed that the IMQZ is composed of oceanic crust based on their observation of subtle linear trends in the second vertical gradient of the total magnetic field intensity within the IMQZ oriented subparallel to the ECMA and BSMA, which could be the result of seafloor spreading.

The OMQZ of the Atlantic JQZ is an approximately 200–350 km wide (west to east) region between the BSMA to M25, becoming narrower from south to north (Figure 1a) (Klitgord & Grow, 1980). Low-amplitude pre-M25 M series magnetic anomalies are not as easily identified in the OMQZ, compared to the M0–M25 anomalies to the east, with only a few studies proposing magnetic anomaly identifications in the OMQZ, such as Barrett and Keen (1976) (M26–M28; north of the New England Seamount Chain) and Bird et al. (2007) (M28, M29, M32, and M40).

M series magnetic anomalies from M0 to M25 are widely accepted in the North Atlantic (Figure 2) (e.g., Bird et al., 2007; Klitgord & Schouten, 1986; Labails et al., 2010; Müller et al., 1997; Schettino & Turco, 2009; Schouten & Klitgord, 1977; Sundvik & Larson, 1988; Tominaga & Sager, 2010a, 2010b; Vogt, 1986), with the magnetic anomaly correlations of most later studies based on the correlations of Klitgord and Schouten (1986). Magnetic anomalies M0–M25 are also widely identified on the conjugate northwest African margin (Klitgord & Schouten, 1986; Labails et al., 2010; Roest et al., 1992; Rona et al., 1970; Verhoef et al., 1990), and some pre-M25 anomalies have been identified (Bird et al., 2007; Roeser et al., 2002), suggesting the Atlantic JQZ does contain correlatable magnetic anomalies.

In addition to the prominent magnetic anomalies (ECMA, BSMA), low-amplitude magnetic anomaly regions (Atlantic JQZ, IMQZ, and OMQZ), and M0–M25 magnetic anomalies, there are distinct, high-amplitude, ellipsoidal magnetic anomalies within the Atlantic JQZ that have not yet been investigated, despite being present in older magnetic anomaly data (Figures 1a and 2) (e.g., Bankey et al., 2002; Klitgord & Behrendt, 1977; Meyer et al., 2016; Zietz, 1982). Two distinct ellipsoidal magnetic anomaly highs, coinciding with the location of the Hudson Fan (hereafter called the Hudson Fan Magnetic Anomaly Highs (HFMAH)), are located ~620 km southeast of the New York Bight, with amplitudes much higher than the surrounding Atlantic JQZ and similar to the magnetic anomalies of Bermuda (Vogt, 1986) and the New England Seamount Chain (Duncan, 1984) (Figures 1a and 2). However, no significant gravity anomaly highs has been identified in conjunction with the HFMAH (Figures 1c and 1d), suggesting that a substantial igneous addition by late-stage magmatism, like Bermuda and the New England Seamount Chain, is unlikely to be the cause of the HFMAH.

### 2.2. Fracture Zones and Tectonic Inheritance at the North Atlantic Margin

Fracture zones, recording approximate plate motion and spreading axis segmentation, are prevalent throughout the North Atlantic and are identifiable by lateral offsets of magnetic anomaly lineations, as well as in gravity and bathymetry data (Figure 1) (Bird et al., 2007; Klitgord & Schouten, 1986; Labails et al., 2010; Müller & Roest, 1992; Schouten & White, 1980; Schettino & Turco, 2009; Tucholke & Schouten, 1988; Vogt et al., 1971). Klitgord and Schouten (1986) determine the locations of fracture zones by offsets in their

identified magnetic anomaly lineations from the Mid-Atlantic Ridge to M25, and extend the trend of these identified fracture zones landward from M25 to the segmentation along the ECMA (Figure 1a). Schettino and Turco (2009) find that the landward extension of these fracture zones in the OMQZ are consistent with the direction of seafloor spreading predicted by their plate reconstruction model, but not further landward to the ECMA through the IMQZ, possibly suggesting an unknown change in seafloor spreading rate and/or direction in the vicinity of the BSMA. Furthermore, Labails et al. (2010) do not find reliable indications of fracture zone directions in the IMQZ.

Many landward extensions of identified fracture zones intersect the margin between ECMA and isostatic gravity anomaly segments (Figure 3a), which may indicate a relation to structural segmentation of the margin during rifting (Behn & Lin, 2000; Klitgord et al., 1988; Wyer & Watts, 2006). The amount of extension during rifting might have been reduced in some areas along the margin from preexisting structural zones of weakness arising from tectonic inheritance (e.g., Manspeizer, 1988; Sheridan et al., 1993). Along margin structural segmentation during continental rifting at the ENAM, represented by segmentation in the ECMA and margin wide isostatic gravity anomaly, is suggested to be the result of variations in both the strength of the continental lithosphere and igneous underplating (Behn & Lin, 2000; Wyer & Watts, 2006) and may be directly related to the formation of incipient fracture zones and the current Mid-Atlantic Ridge segmentation (e.g., Behn & Lin, 2000; Dunbar & Sawyer, 1989; Sawyer, 1985).

### 2.3. ENAM Formation Scenarios

Continental rifting and early Atlantic opening forming the ENAM was diachronous, with the rifting to seafloor spreading transition occurring earlier offshore the southeastern United States (~200 Ma) than offshore Canada (~185 Ma) (Klitgord & Schouten, 1986; Kneller et al., 2012; Manspeizer, 1988; Withjack et al., 1998). The southern ENAM (south of Nova Scotia) experienced voluminous magmatism during rifting, creating a volcanic margin, while to the north of Nova Scotia, the margin transitions from volcanic to nonvolcanic, marked by the termination of the ECMA and SDRs (Biari et al., 2017; Keen & Potter, 1995a, 1995b; Kelemen & Holbrook, 1995; Mchone, 2000; Van Avendonk et al., 2006).

There have been two major scenarios proposed for the ENAM and early Atlantic formation: (1) a ridge jump (or two ridge jumps) (Bird et al., 2007; Klitgord & Schouten, 1986; Kneller et al., 2012; Schettino & Turco, 2009; Vogt, 1973; Vogt, 1986) or (2) a drastic change in spreading rate and direction (Labails et al., 2010; Sahabi et al., 2004). The origin of the BSMA differs in each of these scenarios. In the eastward ridge jump from within the IMQZ to the BSMA scenario, the BSMA would be formed by either the basement relief associated with the juxtaposition of crust the age of the ridge jump with comparatively older crust at the eastern edge of the IMQZ (Klitgord & Grow, 1980), or by a sliver of the African margin continental crust and igneous intrusives isolated by the ridge jump (Vogt, 1973). Alternatively, in the drastic change in seafloor spreading rate and direction scenario, the BSMA would be formed by the basement relief associated with this spreading change (Labails et al., 2010). In addition to the suggested BSMA ridge jump, Bird et al. (2007) adds a second, westward ridge jump in the OMQZ between 164 and 159 Ma, possibly corresponding with the onset of seafloor spreading in the Gulf of Mexico (Van Avendonk et al., 2015).

Half spreading rates used in kinematic plate reconstructions of the early Atlantic vary based on the model, the magnetic anomalies identified, and/or the geomagnetic polarity timescale used (Table 1) (e.g., Bird et al., 2007; Klitgord & Schouten, 1986; Labails et al., 2010; Schettino & Turco, 2009; Tominaga & Sager, 2010a, 2010b). Seafloor spreading rates from M0 to M25 were found using the age assignments and distances between magnetic anomalies, while seafloor spreading rates in the Atlantic JQZ were estimated by either assuming the M21–M25 rate continues landward (Klitgord & Schouten, 1986), using stage pole rotations in plate-scale tectonic reconstructions to geometrically fit conjugate magnetic anomalies and the continents (Labails et al., 2010; Schettino & Turco, 2009), or using magnetic anomaly correlations where available in the OMQZ (Bird et al., 2007).

## 3. Methods

### 3.1. Magnetic Data Acquisition

In this study, we integrated both recently collected (Arsenault et al., 2017) and archived magnetic anomaly data from the NCEI (Figure 2a). The archived magnetic data from the NCEI includes data from 39 cruises

**Table 1**
*Proposed Half Spreading Rates for the Early Atlantic Compiled From Previous Studies (Bird et al., 2007; Klitgord & Schouten, 1986; Labails et al., 2010; Schettino & Turco, 2009; Tominaga & Sager, 2010a, 2010b)*

| Proposed half spreading rates for the early Atlantic | | |
|---|---|---|
| Publication | Chron/age | Half spreading rate |
| Klitgord and Schouten (1986) | 170 Ma (BSMA ridge jmp) to 150 Ma (M21) | 19 mm/yr |
| Klitgord and Schouten (1986) | 150 Ma (M21) to 141 Ma (M16) | 10 mm/yr |
| Klitgord and Schouten (1986) | 141 Ma (M16) to 132 Ma (M10 N) | 7 mm/yr |
| Klitgord and Schouten (1986) | 132 Ma (M10N) to 126 Ma (M4) | Variable |
| Klitgord and Schouten (1986) | 126 Ma (M4) to 118 Ma (M0) | 9 mm/yr |
| Bird et al. (2007) | ~167.5 Ma (M40) to ~154 Ma (M25) | 19.2 mm/yr |
| Bird et al. (2007) | ~154 Ma (M25) to ~120.6 Ma (M0) | 14.4 mm/yr |
| Schettino and Turco (2009) | 200 Ma to 185 Ma (proposed ridge jump) | 4.1 mm/yr |
| Schettino and Turco (2009) | 185 Ma to 147.7 Ma (M21) | 5.45 mm/yr |
| Schettino and Turco (2009) | 147.7 Ma (M21) and younger | 22 mm/yr |
| Labails et al. (2010) | 190 Ma–170 Ma (BSMA) | 8 mm/yr |
| Labails et al. (2010) | 170 Ma (BSMA) to ~154 Ma (M25) | 17 mm/yr |
| Labails et al. (2010) | ~154 Ma (M25) to ~150 Ma (M22) | 27 mm/yr |
| Labails et al. (2010) | ~150 Ma (M22) to ~125 Ma (M0) | 13 mm/yr |
| Tominaga and Sager (2010a, 2010b) | ~154 Ma (M25n) to ~148 Ma (M21n) | 32.6 mm/yr |
| Tominaga and Sager (2010a, 2010b) | 147.5 Ma (M20r) to ~140 Ma (M16n) | 18.4 mm/yr |
| Tominaga and Sager (2010a, 2010b) | ~139 Ma (M15) to ~131 Ma (M6) (AMSZ) | 9.5 mm/yr |
| Tominaga and Sager (2010a, 2010b) | ~131 Ma (M6) and younger | 22.9 mm/yr |

throughout the ENAM that we corrected for the International Geomagnetic Reference Field (IGRF-11 model, Finlay et al., 2010), providing extensive coverage of the study region. We also used the Decade of North American Geology (Zietz, 1982) and North American Magnetic Anomaly Group (Bankey et al., 2002) aeromagnetic total magnetic field data, along with the high-quality EMAG2v3 (version 3) global magnetic anomaly grid composed of a wide range of satellite, aeromagnetic, and shipboard magnetic data that has recently been made available (Meyer et al., 2016) (Figures 1a and 2).

During MCS acquisition on the R/V *Marcus G. Langseth* cruises MGL1407, MGL1408, and MGL1506 along the ENAM, sea surface total magnetic field data were acquired using a Geometrics G882 cesium vapor marine magnetometer (Arsenault et al., 2017). The magnetometer was towed behind the ship navigation reference point at a distance of 253 m (MGL1407 and MGL1408) or 160 m (MGL1506). Sea surface total magnetic field data were also collected during the recent R/V *Neil Armstrong* cruise AR1-06 using a SeaSPY Overhauser magnetometer towed at a distance of 227 m. To obtain the sea surface crustal magnetic anomalies, the raw sea surface total magnetic field data collected during these cruises was corrected for (i) navigation offset from ship-to-magnetometer layback, (ii) outlying data points, (iii) the international geomagnetic reference field (IGRF-11 model, Finlay et al., 2010), and (iv) diurnal field variations (NASA Stennis Space Center Magnetic Observatory, MS). Significant portions of the data collected during these cruises were on long, continuous, margin perpendicular segments that provide high-quality profiles ideal for studying magnetic anomalies produced by seafloor spreading.

### 3.2. Magnetic Anomaly Correlation

We organized straight-line profiles oriented approximately perpendicular to the margin from all of the available sea surface magnetic anomaly data (Figure 2a) and integrated them with the aeromagnetic and EMAG2v3 magnetic anomaly data in Quantum GIS (QGIS Development Team, 2015) to produce a comprehensive, georeferenced data set of the region (Data Set S1). Using this georeferenced data set, we correlated magnetic anomalies on the ENAM by qualitatively matching the character (i.e., amplitude, spacing, and shape) of individual magnetic anomalies on adjacent sea surface magnetic anomaly profiles, using the aeromagnetic and EMAG2v3 magnetic grids to connect the correlated magnetic anomalies to produce lineations (Figures 2, 3b, 3c, and 4). An example of this process for the IMQZ near Cape Hatteras is shown in Figure 3b.

We further selected seven sea surface magnetic anomaly profiles from the data set (Profiles 1–7), concatenating multiple segments, together to cover the latitudinal and longitudinal extent of the ENAM seafloor (see

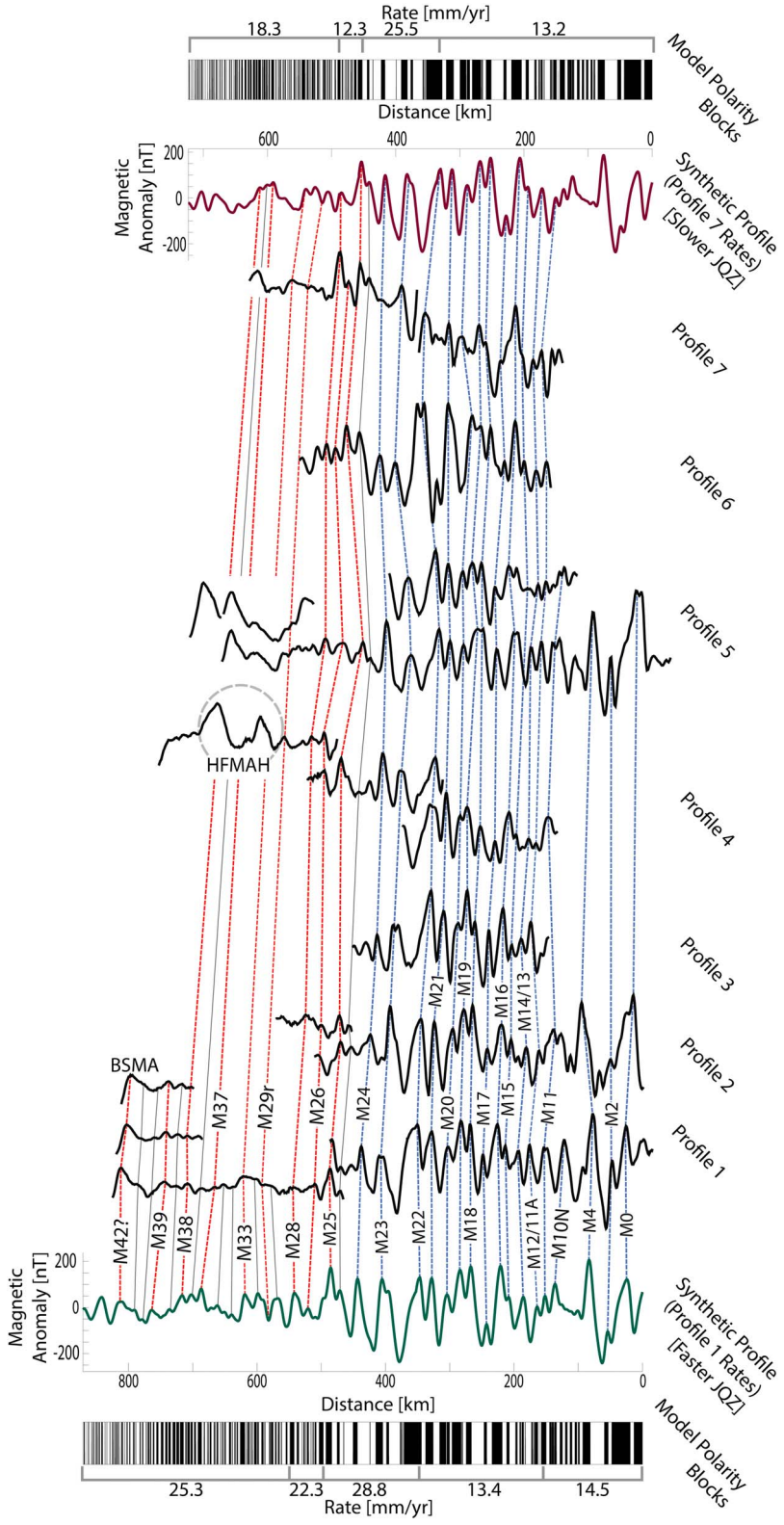


**Figure 4.** Correlation of magnetic anomalies for Profiles 1–7 (Figure 2a) with synthetic magnetic anomaly profile from Pacific M series magnetic polarity block models and the 2012 geomagnetic polarity time scale (Ogg, 2012). Synthetic profile created using half spreading rates estimated for Profile 1 (bottom—green line) and Profile 7 (top—maroon line) (Table 2). Dashed lines show magnetic anomaly correlations (red—OMQZ; blue—M0–M25). Profiles 1, 2, 4, 5, and 7 consist of multiple profiles concatenated together (see Figure 2). Chron numbers labeled.

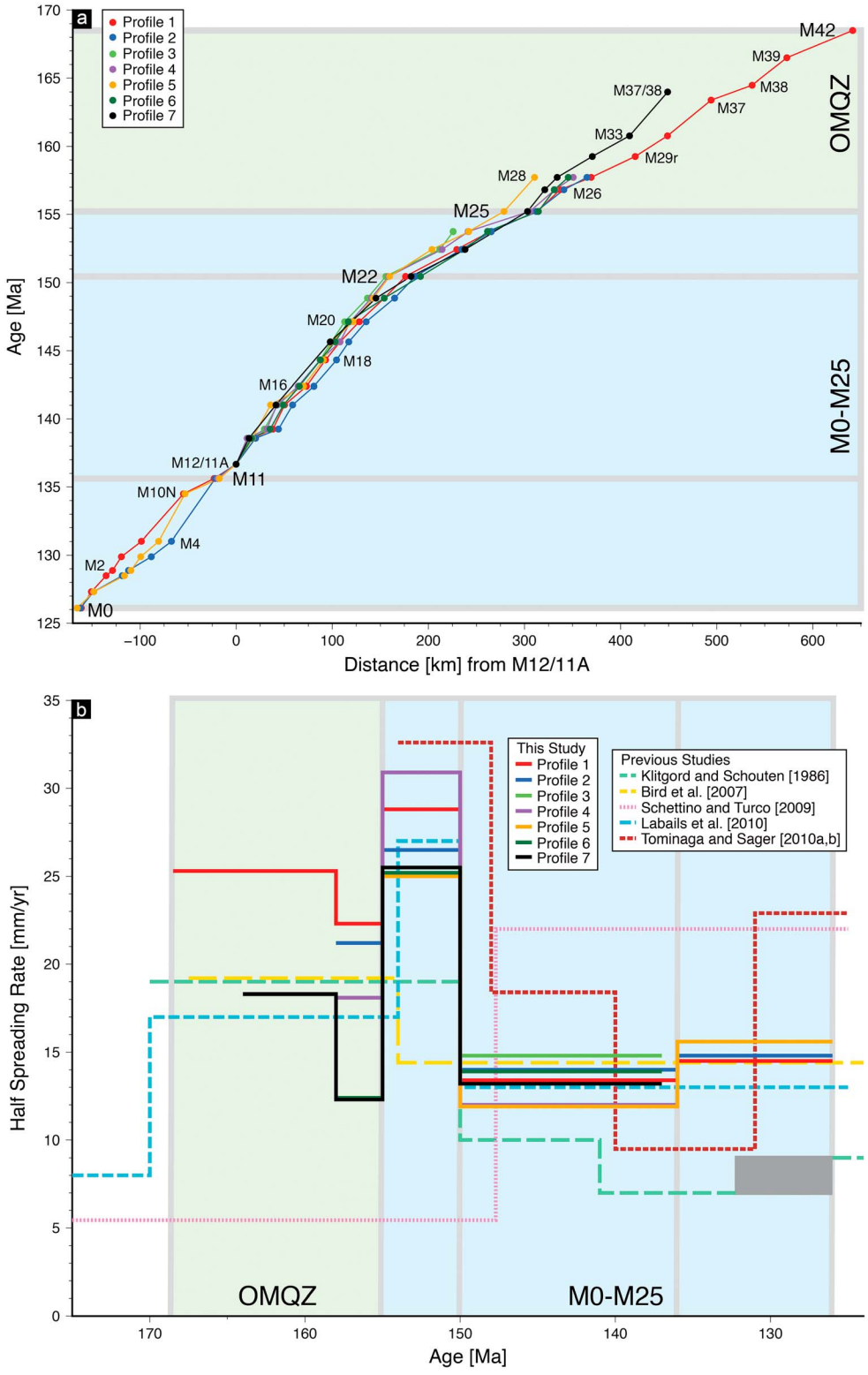


**Figure 5.** (a) Plot of age versus distance for magnetic anomalies. Blue and green backgrounds indicate M0-M25 and OMQZ regions, respectively. Distance expressed relative to M12/M11A (youngest chron present on all seven profiles). (b) Comparison of half spreading rates for this study (solid lines) and previous studies (dashed lines) (Bird et al., 2007; Klitgord & Schouten, 1986; Labails et al., 2010; Schettino & Turco, 2009; Tominaga & Sager, 2010a, 2010b) (Tables 1 and 2). Blue and green backgrounds indicate M0–M25 and OMQZ regions, respectively. Gray box denotes period of variable asymmetric spreading from M10N to M4 in Klitgord and Schouten (1986). (modified from Labails et al., 2010)

Profiles 1, 2, 4, 5, and 7 in Figures 2 and 4). The profiles were oriented as close to perpendicular to the margin as available to best display the character (i.e., amplitude, spacing, and shape) of magnetic anomalies that would be expected from seafloor spreading processes (Figures 2 and 4). We used Profiles 1–7 to assign chron numbers and corresponding ages to the magnetic anomalies using the 2012 Geomagnetic Polarity Time Scale (Ogg, 2012), and to calculate spreading rates for the ENAM.

### 3.3. Magnetic Polarity Block Modeling

We created synthetic magnetic anomaly profiles using the Parker (1973) Fourier summation approach to determine ages for our identified magnetic anomalies. We used a magnetization distribution based on Pacific M series magnetic polarity block models, a basement depth of 8 km (Tucholke, 1986), various half spreading rates (7–30 mm/yr), and paleo-inclinations (34.2° to 44.5°) and declinations (−18.4° to −8.1°) estimated for the early Atlantic using the method of Schettino (2014) and the paleopoles of Schettino and Scotese (2005). We correlated these synthetic magnetic anomaly profiles with Profiles 1–7 to assign chron numbers and ages to our identified magnetic anomalies using the 2012 Geomagnetic Polarity Time Scale (Ogg, 2012) (Figure 4). With the spacing and assigned ages for the magnetic anomalies, we estimated spreading rates for Profiles 1–7 to evaluate the variation both along the margin and over time (Figure 5). Using the estimated spreading rates, final synthetic profiles were created that best matched the observed magnetic anomalies of the region (Figure 4).

### 3.4. Other Geophysical Data

To ensure our identified magnetic anomalies were produced by seafloor spreading processes, rather than secondary magmatic events that could significantly alter the observed magnetic anomaly signal (e.g., seamounts), we acquired and examined the latest satellite-derived gravity (Sandwell et al., 2014) and bathymetry (Andrews et al., 2016; Amante & Eakins, 2009; Butman et al., 2006) data (Figure 1). For Profiles 1, 2, and 4, MCS data were available (MGL1407 Lines 2, 3, 11A, and 13–15) to investigate whether any secondary magma additions and/or significant structural boundaries exist in the subsurface (Arsenault et al., 2017).

## 4. Results

### 4.1. ENAM Magnetic Anomaly Correlations

We assigned chron numbers and ages to 21 of the known anomalies between M0 and M25 (Figures 2b and 4). Additionally, we assign chron numbers to eight previously unidentified magnetic anomalies in the OMQZ, where few previous studies have identified magnetic anomalies (e.g., Barrett & Keen, 1976; Bird et al., 2007), and identify five correlatable magnetic anomalies in the IMQZ (Figure 4 and Table 2).

In the IMQZ, we correlated five low-amplitude magnetic anomalies approximately parallel to both the ECMA and BSMA from 31° to 40°N that have not previously been correlated or discussed, denoted as inner magnetic anomalies (IMA) 1–5 from east to west (Figures 2b, 3b, and 3c). The correlations were made qualitatively by matching the character of IMA1–IMA5 on margin perpendicular profiles crossing the IMQZ (Figure 3c). From 31° to 33.5°N, the magnetic anomaly peak denoted as IMA2 splits into two peaks with an intervening trough (Figures 2b, 3b, and 3c). In the middle of the IMQZ, between 36° to 39°N, the linear magnetic anomalies are less coherent and there are low-amplitude, circular magnetic anomaly highs seaward of the bend in the ECMA that partially obscure the linear magnetic anomalies and mark the location of a change in magnetic anomaly lineation strike and clarity, with more distinguishable lineations with a strike of ~30° to the south and less distinguishable lineations with a strike of ~70° to the north (Figures 1a and 2b). Despite this less coherent middle section between 36° and 39°N where the linear anomalies are more difficult to follow, the consistent character of IMA1–IMA5 and presence of five distinct magnetic anomalies throughout the IMQZ suggests that these IMQZ magnetic anomalies continuously span the entire study area from 31° to 40°N.

Lateral offsets of IMA1–IMA5, striking east/west in the southern IMQZ and northwest/southeast in the northern IMQZ, were interpreted throughout the IMQZ based on the combination of the sea surface magnetic anomaly data and the aeromagnetic and EMAG2v3 magnetic grids in our georeferenced data set (Figures 2b and 3b and Data Set S1). These offsets were consistently oriented perpendicular to IMA1–IMA5, striking east/west in the southern IMQZ and northwest/southeast in the northern IMQZ (Figures 2b, 3a, and 3b). Many of these IMQZ offsets documented in this study appear to intersect the ECMA at gaps between

**Table 2**
*Half Spreading Rates Estimated in This Study at Seven Profiles Along the Margin (See Figure 2 for Locations and Figure 5b for Comparison)*

| | | Half spreading rate (mm/yr) | | | | | | |
|---|---|---|---|---|---|---|---|---|
| Chron range | Age range (Ma) | Profile 1 | Profile 2 | Profile 3 | Profile 4 | Profile 5 | Profile 6 | Profile 7 |
| M0–M11 | 126–136 | 14.5 | 14.8 | | | 15.6 | | |
| M11–M22 | 136–150 | 13.4 | 14.0 | 11.3 (M12–M22) | 12.0 | 11.9 | 13.9 (M12–M22) | 13.2 (M12–M22) |
| M22–M25 | 150–155 | 28.8 | 26.5 | | 30.9 | 25.0 | 25.2 | 25.5 |
| M25–M28 | 155–158 | 22.3 | 21.2 | | 18.1 | | 12.4 | 12.3 |
| M28–M42[a] | 158–168.5 | 25.3 | | | | | | |
| M28–M37/38[b] | 158–164 | | | | | | | 18.3 |

[a]Chron range only available on Profile 1. [b]Chron range only available on Profile 7.

individual segments (Figure 3a), and they often line up with previously identified traces of fracture zones extending through the OMQZ and M0–M25 (Figures 2b, 3a, and 3b) (Klitgord & Schouten, 1986).

Throughout the OMQZ, we correlated magnetic anomalies despite the low-amplitude characteristic of the Atlantic JQZ (Figure 2b). Similar to the ECMA, IMA1-IMA5, and the BSMA, there is a change in magnetic anomaly lineation strike on the west side of the OMQZ, but this change becomes less pronounced moving to the east. The magnetic anomaly lineations consistently have a strike of ~30° in the south, and in the north the strike varies from ~70° to ~55°, from west to east, in the north (Figure 2b). Additionally, the OMQZ is wider in the south (~360 km at 31°N), becoming narrower moving northward (~220 km at 37°N), which corresponds to a wider magnetic anomaly lineation spacing in the south compared to the north (Figure 2b). The middle portion of the OMQZ (approximately 34°–37°N) has multiple ellipsoidal magnetic anomaly highs and lows, including the HFMAH, which created difficulty in correlating magnetic anomalies (Figure 2).

We propose the existence of correlatable magnetic anomalies older than M25 in the OMQZ. Based on our synthetic profiles, we identified M series magnetic anomalies M26, M28, M29r, M33, M37, M38, and M39 in the Atlantic JQZ (Figures 2b and 4 and Table 2). Additionally, the magnetic anomaly character of the BSMA on recently collected sea surface magnetic anomaly profiles (from MGL1407 and MGL1408) is similar to that of M42 (~168.5 Ma) in our synthetic profile, with a steep amplitude increase to the magnetic anomaly peak on the west, followed by a more gradual tapering off of amplitude moving to the east (see Profile 1 in Figures 2 and 4). In the MCS data, satellite-derived gravity anomaly, and satellite-derived bathymetry data available for our profiles, only one significant seamount was identified, on the west end of MGL1407 Line 11A (Profile 2 in Figures 2b and 4) (Arsenault et al., 2017), which does not appear to affect the magnetic anomaly signal given the excellent correlation with other profiles nearby along which the absence of seamounts is confirmed (e.g., MGL1407 Line 13; Profile 1 in Figures 2b and 4).

We have identified coherent, correlatable magnetic anomalies from east of the OMQZ to Bermuda in the area where chrons M0–M25 have previously been identified (Figure 2). Between M0 and M25, we identified M0–M4 and M10N–M25, with magnetic anomaly peaks corresponding to M11A and M12, M13 and M14, and M24A, M24B, and M25 merging together due to the slow seafloor spreading (Figure 4 and Table 2). Magnetic anomalies M5–M10 were not distinguishable due to the close proximity of magnetic anomalies M4 and M10A (Figures 2a and 4).

### 4.2. OMQZ and M0–M25 Seafloor Spreading Rates

We documented the spatial and temporal variation in seafloor spreading rates, both in the OMQZ and from M0 to M25, using the age assignments and magnetic anomaly spacing on Profiles 1–7 (oriented as close to perpendicular to the margin from the data available) (Figure 5 and Table 2). We divided the OMQZ into two age ranges: (1) M28 to M25 (~158–155 Ma) and (2) pre-M28. M28 to M25 seafloor half spreading rates varied along the margin, with a value of ~20 mm/yr for Profiles 1, 2, and 4 in the south and middle of the OMQZ, decreasing to ~12.3 mm/yr for Profiles 6 and 7 in the north (Figure 5 and Table 2). Pre-M28 half spreading rates were 25.3 mm/yr from M42 to M28 (~168.5–158 Ma) on Profile 1 and 18.3 mm/yr from M37/38 to M28 (~164–158 Ma) for Profile 7 (Figure 5 and Table 2).

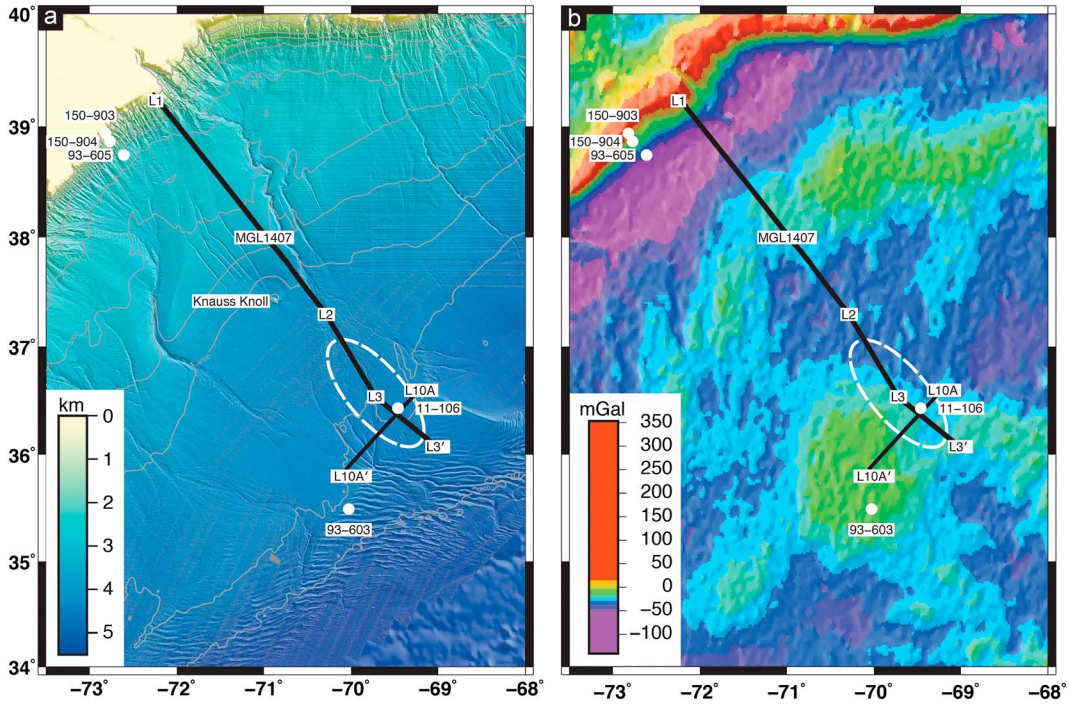


**Figure 6.** (a) Bathymetry in the vicinity of the HFMAH (Butman et al., 2006). White dashed line outlines HFMAH location (see Figure 2). Gray contours every 500 m. White circles denote locations of Deep Sea Drilling Program sites. Knauss Knoll location labeled (Lowrie & Heezen, 1967). (b) Gravity anomaly grid in the vicinity of the HFMAH (Sandwell et al., 2014). White dashed line outlines HFMAH location (see Figure 2). White circles denote locations of Deep Sea Drilling Program sites.

To understand the temporal variation in seafloor spreading, we divided M0–M25 into three age ranges based on inflection points in the age-distance plot (Figure 5a): (1) M25 to M22 (~155–150 Ma), (2) M22 to M11 (~150–136 Ma), and (3) M11 to M0 (~136–126 Ma). From M25 to M22, half spreading rates were estimated at ~25–31 mm/yr (Profiles 1, 2, 4–6) (Figure 5 and Table 2). At M22, the half spreading rate slowed, with estimated half spreading rates of ~12–14 mm/yr (Profiles 1–7) from M22 to M11 (or M12 when M11 was not identified) (Figure 5 and Table 2). The half spreading rate from M11 to M0 was estimated at ~15 mm/yr (Profiles 1, 2, and 5) (Figure 5 and Table 2). During all three age range divisions from M0 to M25, the seafloor spreading rates were similar on Profiles 1–7, not varying along the margin.

### 4.3. Anomalous Magnetic Features in the ENAM

In addition to the well-known magnetic anomaly features such as the ECMA and BSMA, and the high-amplitude magnetic anomalies associated with the New England Seamount chain and Bermuda, there are multiple distinct, high-amplitude, ellipsoidal magnetic anomalies, including the HFMAH, which have not been previously investigated despite being of similar amplitude to the ECMA, New England Seamount Chain, and Bermuda (Figure 1a). No major magmatic and/or structural disturbances were imaged by the MCS data in the crust, nor are there bathymetry or gravity anomaly highs present in conjunction with the HFMAH (Figures 6a, 6b, 7b, and 7c). MGL1407 MCS Lines 2, 3, and 10A over the HFMAH showed seafloor, basement, and Moho reflectors at approximately 4.4 km, 10.3 km, and 18.6 km, respectively (Figures 7b and 7c). Two zones of rough basement topography, with variations up to ~400 m, were observed in the MCS data of MGL1407 MCS Lines 2 and 3 below the two peaks of HFMAH (Figure 7b). In addition, MGL1407 MCS Line 10A, which crosses Line 3, shows that these zones of rough basement topography are three-dimensional in structure (Figures 7b and 7c).

## 5. Discussion

The correlation of marine magnetic anomalies has played a prominent role in understanding the seafloor spreading history of the ENAM (e.g., Bird et al., 2007; Klitgord & Schouten, 1986; Labails et al., 2010;

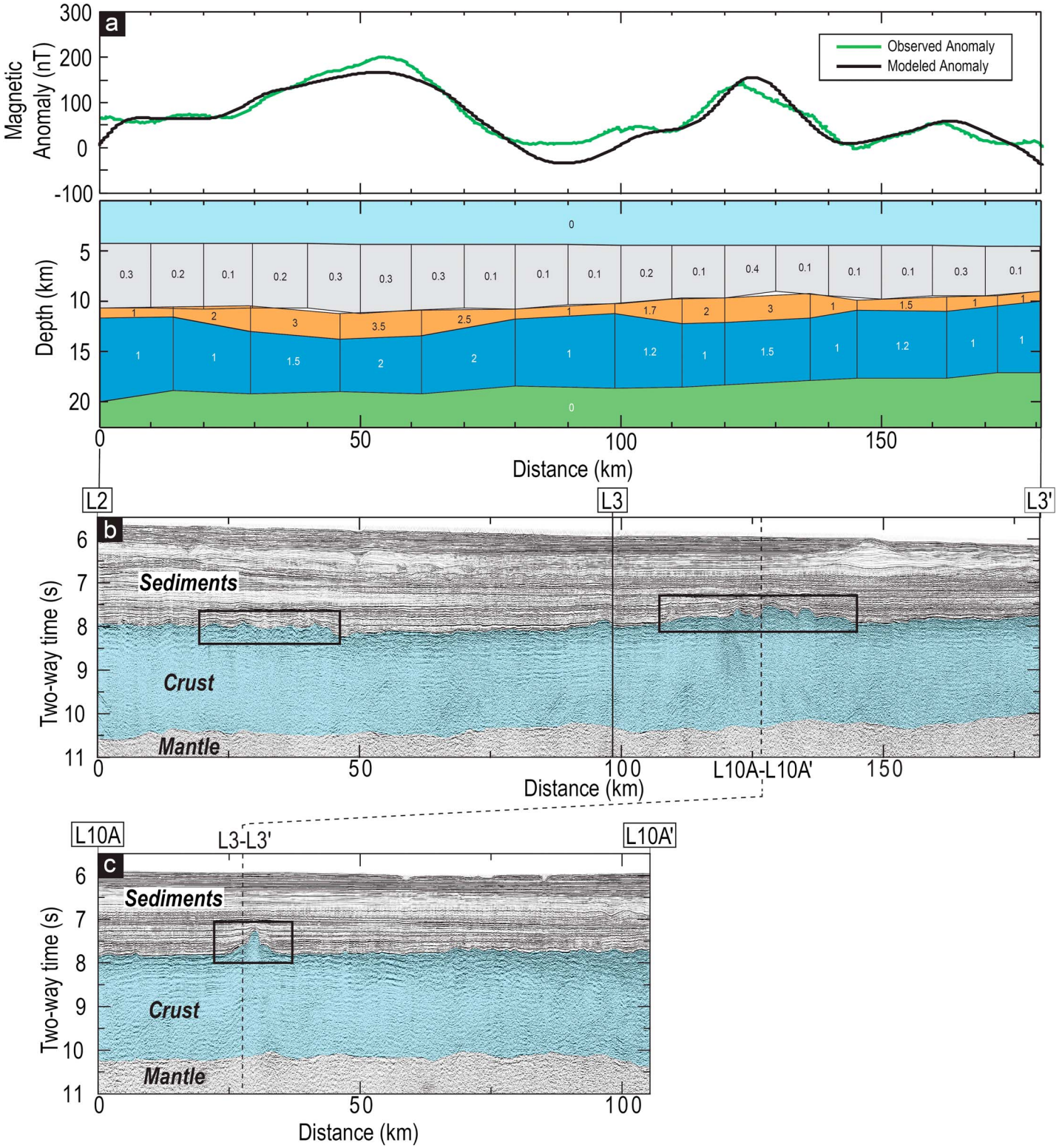


**Figure 7.** (a) Magnetic forward model varying both layer 2/3 thickness and magnetization for MGL1407 lines 2 and 3 (see Figure 6 for location). Green line is observed magnetic anomaly in MGL1407 sea surface data (Arsenault et al., 2017); black line is calculated magnetic anomaly from model (top) . Prism geometry used in forward model showing water (light blue), sediment (gray), layer 2 (orange), layer 3 (blue), and mantle (green), with magnetizations (A/m) for each prism marked (~2:1 vertical exaggeration) (bottom). (b) MCS data for MGL1407 lines 2 and 3 (see Figure 6 for location) (Arsenault et al., 2017) showing sediment, crust, and mantle. Dashed line shows line 10A crossing. Black boxes mark areas of rough basement topography. (c) MCS data for MGL1407 line 10A (see Figure 6 for location) (Arsenault et al., 2017) showing sediment, crust, and mantle. Dashed line shows line 3 crossing. Black box marks area of rough basement topography.

Schettino & Turco, 2009; Tominaga & Sager, 2010b). Our M0–M25 magnetic anomaly identifications reconfirm those from previous studies (e.g., Klitgord & Schouten, 1986; Labails et al., 2010), including the M25 location proposed by Labails et al. (2010) north of 35.5°N, which is at an anomaly ~50 km to the east of the M25 previously proposed by Klitgord and Schouten (1986) (Figures 2b and 4). While we confirm the slow spreading regime from M0 to M25 (~126–155 Ma), found in previous studies (Figure 5 and Table 1) (Bird et al., 2007; Klitgord & Schouten, 1986; Labails et al., 2010; Schettino & Turco, 2009; Tominaga & Sager, 2010a, 2010b), our comprehensive magnetic anomaly and geophysical data analyses provided an unprecedented opportunity to closely investigate seafloor spreading rates and directions in the Atlantic JQZ. From these results, we are able to propose a scenario for the early Atlantic opening, including the possible influence of preexisting margin structure and rifting segmentation, and the subsequent seafloor spreading history forming the ENAM.

### 5.1. Early ENAM Seafloor Spreading Regimes

We identify three regions within the Atlantic JQZ with different seafloor spreading regimes between the ECMA and M25 based on notable differences in magnetic anomaly coherency, magnetic anomaly lineation strike, and seafloor spreading rates (Figures 2b, 5 and Table 2): (1) offshore New York and Massachusetts (New England Region); (2) offshore Virginia and New Jersey (Mid-Atlantic Region); and (3) offshore North and South Carolina (Carolina Region). In addition, the IMQZ, the previously identified area with low-amplitude magnetic anomalies between the ECMA and BSMA (Vogt et al., 1971) extends south to north along the margin across these three Atlantic JQZ regions (Figure 2a). We suggest these differences indicate that each region underwent different spreading regimes during the formation of the Atlantic JQZ, including accommodating the transitioning from the prominent bend characteristic of the ECMA offshore the New York Bight to the more linear strike at M25 (Figure 2) that necessitates the emplacement of an additional ~28,000 $km^2$ of seafloor.

The New England Region extends ~470 km from east to west in its center at 38°N, with its northern boundary at the New England Seamount Chain and its southern boundary located offshore the New York Bight, near the prominent strike change in the ECMA and BSMA (Figure 2a). Both the IMQZ and OMQZ sections of this region widen longitudinally from north to south (Figure 2a). The magnetic anomalies in the New England Region are semicoherent, and there is a change in magnetic anomaly lineation strike occurring from west to east across this region, being ~80° at the ECMA, ~70° at the BSMA, and ~55° at M25, suggesting a counterclockwise reorientation of the paleomagmatic center during formation (Figure 2b). Estimated half spreading rates in the New England Region in the OMQZ were 18.3 mm/yr from M37/38 to M28 and ~12.3–18.0 mm/yr from M28 and M25, being lower in north (Figure 5b and Table 2).

The Mid-Atlantic Region extends ~620 km from east to west in its center at 36°N, with its northern boundary located offshore the New York Bight and its southern boundary located offshore Cape Hatteras, North Carolina (Figure 2a). The magnetic anomalies in the Mid-Atlantic Region are the least coherent of the three regions, particularly in the OMQZ, and there is an approximately consistent magnetic anomaly lineation strike of 30° across this region, suggesting little region wide reorientation of the paleomagmatic center during formation (Figure 2b). The estimated half spreading rate in the Mid-Atlantic Region in the OMQZ was ~18.0 mm/yr from M28 to M25 (Figure 5b and Table 2).

The Carolina Region extends ~575 km from east to west in its center at 32°N, with its northern boundary located offshore Cape Hatteras, North Carolina, and the southern boundary located offshore southern South Carolina and the southern termination of the ECMA (Figure 2a). The IMQZ in the Carolina Region is approximately consistent in width, while the OMQZ widens slightly longitudinally from north to south (Figure 2a). The magnetic anomalies in the Carolina Region are the most coherent of the three regions, and there is an approximately consistent magnetic anomaly lineation strike of 30° across this region (Figure 2b). Estimated half spreading rates for the Carolina Region in the OMQZ were 25.3 mm/yr from M42 to M28 and 22.3 mm/yr from M28 to M25 (Figure 5b and Table 2).

We further examine the along-margin differences in the Atlantic JQZ seafloor spreading regimes between the BSMA and M25 for the first time (Figures 2a and 4). While we confirm that the spreading rates calculated from Profiles 1–7 are consistent with previous estimates from M0 to M25 (Figure 5b and Tables 1 and 2) (e.g., Bird et al., 2007; Klitgord & Schouten, 1986; Labails et al., 2010; Schettino & Turco, 2009), we find that the seafloor spreading rates in the OMQZ of the ENAM are slower in the north (~12 mm/yr on Profiles 6 and 7) compared

to the south and middle (~20 mm/yr on Profiles 1, 2, and 4) and are also slower than the rates calculated for the conjugate West African Margin (half spreading rates of 22.0 mm/yr and 24.6 mm/yr in Roeser et al., 2002 and Bird et al., 2007, respectively). Furthermore, our new identification of M series anomalies in the Atlantic JQZ are in agreement with the M28 and M29 of Bird et al. (2007), while we confidently redefine M33 and M39 instead of the previously identified M32 and M40, respectively (Bird et al., 2007), based on our detailed investigation of the superposed anomalies produced by remnant magnetization in crust formed from slower spreading during a period of rapid polarity reversals and our use of an updated, more recent geomagnetic polarity timescale (2012 geomagnetic polarity timescale (Ogg, 2012)) (Figures 4 and S1). Based on their interpreted duplicates of chrons M32–M38 on the West African Margin and absence on the ENAM, Bird et al. (2007) proposed a major westward ridge jump within the OMQZ. However, the presence of M33, M37, and M38 in this study (Figures 2 and 4) suggests that seafloor spreading between the BSMA and M25 occurred without this specific proposed ridge jump, consistent with previous studies (e.g., Klitgord & Schouten, 1986; Labails et al., 2010; Schettino & Turco, 2009), though we are unable to definitively rule out the presence of ridge jumps that could have occurred between our interpreted magnetic anomalies.

Along the margin in the IMQZ, throughout all three Atlantic JQZ regions, our systematic investigation of magnetic anomaly correlations enables us to discover five coherent, correlatable magnetic anomalies IMA1–IMA5 extending along the margin in the IMQZ throughout all three Atlantic JQZ regions (Figure 2b, 3b, and 3c). We propose that the coherency of these linear magnetic anomalies is attributed to either (1) synrift, extensional stage magmatism emplaced in stretched continental or transitional crust similar to what is seen in rift setting around the world (e.g., Bridges et al., 2012; Bronner et al., 2011; Gunn, 1997; Russell & Whitmarsh, 2003) or (2) steady state mid-ocean ridge magmatism forming the earliest oceanic crust of the Atlantic (e.g., Bird et al., 2007; Klitgord & Schouten, 1986; Labails et al., 2010; Schettino & Turco, 2009).

Although IMA1–IMA5 are distinctive and correlatable along the entire margin, assigning ages/chron numbers to IMA1–IMA5 and calculating seafloor spreading rates are currently challenging. In either the proposed ridge jump (Bird et al., 2007; Klitgord & Schouten, 1986; Kneller et al., 2012; Schettino & Turco, 2009; Vogt, 1973) or change in spreading rate and direction (Labails et al., 2010) early opening scenarios, the IMQZ formation predates the BSMA. The estimated age for the BSMA from previous studies is ~168–171 Ma (e.g., Benson, 2003; Klitgord & Schouten, 1986), and if the BSMA source is crust produced by seafloor spreading, it may be M42 (~168.5 Ma) based on the similarity in magnetic anomaly character (Figure 4). These BSMA ages are near the age of the oldest chron in the M series of the geomagnetic polarity timescale (~171 Ma) (Ogg, 2012). Consequently, the IMQZ formation prior to the BSMA predates the timescale, which currently precludes us from assigning ages/chon numbers to IMA1–IMA5. The lateral offsets of IMA1–IMA5 in the Carolina and Mid-Atlantic Regions documented in this study coincide with predicted extensions of fracture zones made by Klitgord and Schouten (1986), while our interpreted offsets in the New England Region trend more toward the north, maintaining an orientation perpendicular to IMA1–IMA5 (Figures 1a and 3a), which is consistent with the findings of Schettino and Turco (2009). Regardless of the mode of IMQZ seafloor formation, the margin-wide presence of IMA1–IMA5 indicates that the igneous activity forming the source of these magnetic anomalies extended along the entire margin during the formation of the IMQZ, recording the contemporaneous geomagnetic field at the time of emplacement.

### 5.2. Tectonic Origin of Anomalous Magnetic Features in the ENAM

In the Atlantic JQZ, there are distinct, high-amplitude, ellipsoidal magnetic anomalies, including the HFMAH at the south end of the New England Region and Mid-Atlantic Region (Figure 1a), that have not been investigated, despite being historically present in magnetic anomaly data (e.g., Bankey et al., 2002; Klitgord & Behrendt, 1977; Meyer et al., 2016; Zietz, 1982). These magnetic anomalies do not exhibit the margin-wide, coherent anomaly character associated with synrift volcanism or seafloor spreading processes (e.g., Bridges et al., 2012; Gunn, 1997; Vogt, 1986) nor are they related to known volcanic features of the ENAM that produce high-amplitude magnetic anomalies of similar dimensions, such as the New England Seamount Chain (Duncan, 1984), Bermuda (Vogt, 1986), the Great Stone Dome (Grow, Klitgord, & Schlee, 1988; Taylor et al., 1968), a buried seamount near the Hudson Canyon (Grow et al., 1988), or Knauss Knoll (Lowrie & Heezen, 1967; Sweeney et al., 2012) (Figures 1, 2, and 6b). Using recently collected high-resolution sea surface magnetic anomaly and MCS data from the HFMAH (Arsenault et al., 2017), we seek to identify the magnetic

source creating the HFMAH and other distinct, high-amplitude, ellipsoidal magnetic anomalies of the ENAM (Figure 1a) based on observations, modeling, and the regional tectonic history of the Atlantic JQZ.

The most obvious marine magnetic anomaly sources are (i) geomagnetic polarity boundaries, (ii) excess volcanic emplacement, and (iii) major lithological and structural boundaries. The HFMAH being sourced to a contrast from geomagnetic polarity reversals is unlikely since the frequent polarity reversals during a period of low geomagnetic field strength thought to occur during the formation of the Atlantic JQZ would produce low-amplitude magnetic anomalies, as seen in the Atlantic JQZ surrounding the HFMAH (Figure 1a) (Larson & Pitman, 1972; Tivey et al., 2006). Furthermore, late-stage magmatic events can emplace excess igneous material producing high-amplitude magnetic anomalies, as seen at the New England Seamount Chain, Bermuda, and the ECMA (Duncan, 1984; Talwani et al., 1995; Vogt, 1986). However, neither the most recent satellite-derived bathymetry, gravity anomaly, and vertical gravity gradient grids nor the MCS data collected for MGL1407 Lines 2, 3, or 10A indicate any local additions of excess igneous material under the HFMAH (Figures 6a, 6b, 7b, and 7c); hence, excess volcanism as the predominant source of the HFMAH is also unlikely.

To investigate the possible magnetic source architecture producing the HFMAH, we conducted two-dimensional magnetic forward modeling (Figure 7a) (Talwani & Heirtzler, 1964) with the source geometry identified beneath the HFMAH using the MCS data from MGL1407 MCS Lines 2 and 3 (Arsenault et al., 2017) and depths estimated with the velocity model of Lizarralde and Holbrook (1997), located ~550 km to the west of the HFMAH. MGL1407 MCS Lines 2 and 3 were selected for this modeling as they cross directly over both peaks of the HFMAH and display the zones of rough basement topography (Figure 7b). To match the calculated and observed magnetic anomaly signal in our forward modeling, we adjusted the magnetization values for layer 2 and 3 and the thickness of layer 2. The corresponding thickness of layer 3 is dependent on the layer 2 thickness since the total igneous crust is constrained by the basement and Moho reflector depths. After producing two end-member models varying only the layer 2 thickness and magnetization, respectively (Figure S2), we created a series of models to include variations in both the layer 2 and 3 thicknesses (1–2.5 km and 5–8 km for layers 2 and 3, respectively) and magnetizations (1 to 3.5 and 1 to 2 A/m for layers 2 and 3, respectively (e.g., Johnson & Pariso, 1993)) (final model shown in Figure 7a). In each model, the most distinctive magnetic source bodies (i.e., highest magnetization and/or thickest layer 2) were confined directly beneath the two peaks of the HFMAH, corresponding with the locations of rough basement topography in the MCS data, suggesting that processes acting to increase the magnetization and/or layer 2 thickness could be responsible for producing the source of the HFMAH (Figure 7).

Differences in the abundance and type of magnetic minerals in the neighboring rock formations create lithological contrasts (with different magnetic susceptibility of each rock formation) that could produce magnetic anomalies. While initial sediment deposition at the ENAM included evaporates and carbonates during the Jurassic, from the Cretaceous to the present, terrigeneous sediments have been deposited by river systems along the coast (Poag & Sevon, 1989). Numerous submarine canyon systems incise the ENAM continental slope, and some have been active over millions of years transporting the terrigeneous sediment from the continental shelf to the abyssal plain (Gardner, 1989; Pilkey & Cleary, 1986) (Figure 1b). The Hudson Fan, coinciding with the location of the HFMAH, receives terrigenous sediments through the Hudson Canyon system forming a thick sedimentary package (Figures 7b and 7c) (Butman et al., 2006; Poag & Ward, 1993). Nearby Deep Sea Drilling Program holes 11 and 106 penetrated the top 1,015 m of sediments on the shelf edge and slope (Figure 6a), manifesting some discrete zones with up to 15 wt % iron and sulfide bearing sediments (Hollister et al., 1972). Although this is a significant weight percentage of possible magnetic carriers, the contribution of the sedimentary magnetization to the total magnetic anomaly amplitude is only ~10% (~10–20 nT) in our forward modeling even if we distribute this concentration of iron-bearing minerals throughout the entire sediment package beneath the two HFMAH peaks. Therefore, the coincidence of the HFMAH and Hudson Canyon locations cannot explain the origin of HFMAH. Additionally, lithological contrasts with a zone of higher magnetization could exist in the igneous basement from hydrothermal alteration processes. In the lower crust and upper mantle at the modern-day Mid-Atlantic Ridge serpentinization processes have been known to produce strongly magnetized crust (e.g., Oufi & Cannat, 2002; Tominaga et al., 2016); however, the MCS data clearly indicate that beneath the two HFMAH peaks, there is no evidence of thin crust, exhumed lower crust and upper mantle, or deep penetrating faults that could promote alteration within the lower crust and upper mantle (Figures 7b and 7c).

Structural boundaries can produce magnetic anomalies, including faults and basement offsets along long-lived fracture zones, some of which have been predicted to extend near the HFMAH (Figure 1a) (e.g., Grauch et al., 2006; Klitgord & Schouten, 1986; Larson & Pitman, 1972). However, the directions of the predicted fracture zone extensions (Klitgord & Schouten, 1986) are perpendicular to the expected direction of a fault or basement offset that could produce the observed two-peak magnetic anomaly high, and there is no evidence in the MCS data of faults or basement structure that is indicative of a fracture zone (Figures 1a, 7b, and 7c) (Grauch et al., 2006; Gudmundsson, 1993).

To explain the origin of the HFMAH based on the combination of the basement morphology beneath the HFMAH and the regional tectonic history, we propose a hypothesis where the HFMAH is attributed to the emplacement of basalts enriched in iron and titanium produced by a short-lived propagating rift, as seen at some modern-day rifting and spreading centers (e.g., Hey, 1977; Hey et al., 1980; Sinton et al., 1983; Wanless et al., 2012). Magnetic anomalies in these areas are characterized by ellipsoidal magnetic anomaly highs that are unrelated to the seafloor spreading magnetic anomalies (e.g., Hey et al., 1980; Hey & Wilson, 1982), suggesting that ellipsoidal magnetic anomalies of the ENAM, such as the HFMAH, could be related to tectonic activity during the early Atlantic seafloor spreading. For a propagating rift, as the growing spreading center advances, the transform fault becomes inactive and it, along with a segment of the dying spreading center, is added to the adjacent oceanic lithosphere (see Figures 8b and 8c insets) (Hey, 1977). The wakes of propagating rifts have been associated with unusually high-amplitude magnetic anomalies, which are correlated to basalts enriched in iron and titanium that create abundant single-domain magnetite from renewed crystal fractionation when the propagating rift breaks through older, thicker crust, or taps off-ridge, relatively differentiated magma chambers (Hey et al., 1980; Horen & Fleutelot, 1998; Sinton et al., 1983; Wanless et al., 2012). Additionally, it has been observed that there is thicker than average extrusive crust, represented by seismic layer 2A, at the propagating rift tip (Bazin et al., 2001; Wanless et al., 2012). The propagating rift also creates short-wavelength, rough basement topography as a result of the change in seafloor spreading rate at the area at the tip of the propagating rift, from zero to the rate present for the rest of the ridge (Hey et al., 1980). Furthermore, short-wavelength, rough basement topography is observed beneath the magnetic anomaly peaks of the HFMAH (Figures 7b and 7c). We suggest that the thickened layer 2 with higher magnetization found in our modeling, confined beneath the two rough basement topography zones, could represent the magmatism emplacing a thicker extrusive layer of highly magnetized basalt, as has been observed at the tips of a propagating rift (Figure 7) (Bazin et al., 2001; Hey et al., 1980, 1986; Miller & Hey, 1986; Wanless et al., 2012; Wilson & Hey, 1995).

### 5.3. Effect of Preexisting Structure and Rift Segmentation on ENAM Crustal Formation

The juxtaposition of accreted terranes from past plate tectonic cycles are generally thought to play a key role in the localization of continental breakup, such as during the rifting of Pangea that led to the formation of the ENAM, with rifting occurring along a preexisting zone of weakness in the continental crust (Dunbar & Sawyer, 1989; Labails et al., 2010; Manspeizer, 1988; Sawyer, 1985; Sheridan et al., 1993; Wilson, 1966). Preexisting structure could also influenced the later crustal formation of the ENAM following the initial rifting, causing rifting segmentation and magmatic center offsets that may have led to the formation of early Atlantic fracture zones (e.g., Behn & Lin, 2000; Sawyer, 1985). Our newly identified patterns of correlated magnetic anomalies and interpreted offsets in the Atlantic JQZ and their apparent coincidence with possible indicators of rifting segmentation and terrane boundaries may support this hypothesized influence from preexisting structure, if the anomaly offsets are representative of incipient fracture zones (Behn & Lin, 2000; Boote & Knapp, 2016; Higgins & Zietz, 1983; Sawyer, 1985; Williams & Hatcher, 1982). One of the most prominent observations of this coincidence is that many of the lateral offsets of IMA1–IMA5 within the IMQZ appear to intersect the ECMA at the gaps between major segments observed in the aeromagnetic and EMAG2v3 magnetic grids (Figures 2b and 3a). The ECMA segmentation is thought to represent along margin rifting segmentation from variations in magmatism and/or preexisting lithospheric weaknesses, which may have led to incipient fracture zone formation (Behn & Lin, 2000; Dunbar & Sawyer, 1989; Wyer & Watts, 2006). The coincidence between the ECMA segmentation and IMA1–IMA5 lineation offsets documented in this study, if they indicate fracture zones, could support the hypothesis that the early pattern of seafloor spreading or synrift magmatism forming the IMQZ seafloor could have been governed by the rifting architecture and pre-existing structure of the margin (Figure 2b) (Behn & Lin, 2000; Dunbar & Sawyer, 1989; Wyer & Watts, 2006).

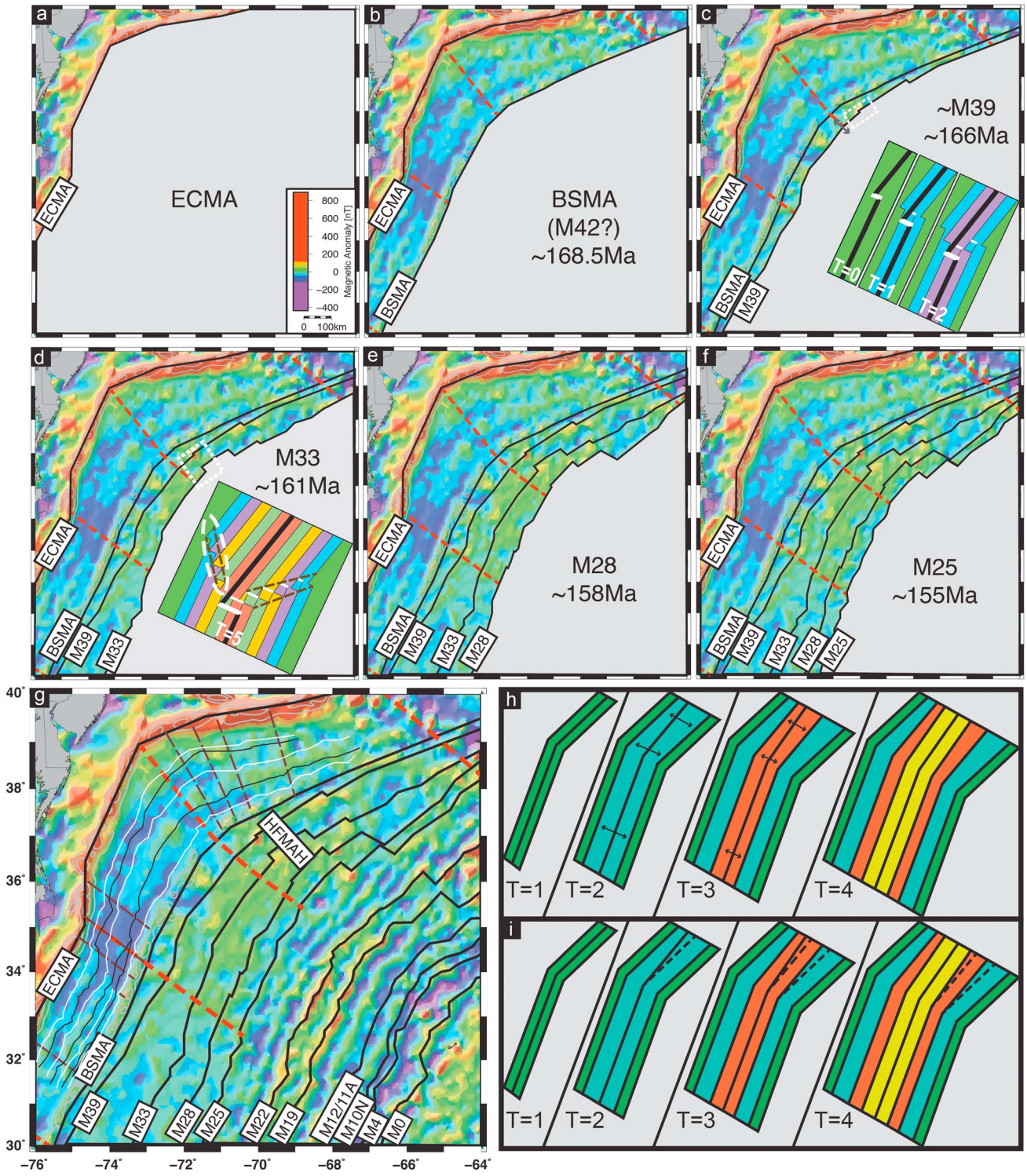


**Figure 8.** Schematic of Atlantic JQZ formation history from ECMA to M25. Magnetic anomaly name or chron number denote seafloor being formed at each time step (a-g), with solid black lines showing inferred ridge location. Arrows show inferred spreading direction for paleo-Mid-Atlantic Ridge. Red dashed lines mark New England, Mid-Atlantic, and Carolina region boundaries (Figure 1). (c and d) White dashed box shows developing HFMAH. (g) Brown dashed lines mark interpreted offsets in IMQZ magnetic anomalies IMA1–5. (h) Schematic showing ridge reorientation over four time steps by asymmetric spreading (indicated by arrow length in $T = 2$ and $T = 3$). (i) Schematic showing ridge reorientation over four time steps by westward ridge jumps in $T = 2$ and $T = 3$, with dashed line indicating ridge location prior to jump. Inset diagrams in panels Figures 8b and 8c detail propagating rift evolution at time steps of 0, 1, 2, and 5: Like color bars represent crust of same age; thick black line is ridge axis; thick white line is active transform fault; thin white line is fossil transform fault; dashed brown lines in $T = 5$ represent "pseudofault" trend, with the white dashed ellipse outlining the corresponding area of potentially high magnetic anomalies, such as those of the HFMAH (modified from Hey, 1977, their Figure 2).

Furthermore, the New England, Mid-Atlantic, and Carolina Region boundaries, identified based on changes in magnetic anomaly character, are observed to coincide with the previously identified predicted extensions of major fracture zones and intersect the ECMA at major gaps between segments that are thought to be related to rifting segmentation and preexisting zones of weakness (Behn & Lin, 2000; Klitgord & Schouten, 1986). The southernmost boundary coincides with the southern termination of the ECMA, as well as the Blake Spur Fracture Zone, which is thought to have formed from at an abrupt change in rheology associated with a suture (Figures 2b and 3a) (Boote & Knapp, 2016; Klitgord & Schouten, 1986; Sawyer, 1985). Likewise, the boundary between the Carolina and Mid-Atlantic Regions coincides with the Northern Kane Fracture Zone (Müller & Roest, 1992; Tucholke & Schouten, 1988), which intersects a major gap between ECMA segments located offshore Cape Hatteras, North Carolina that also approximately coincides with the boundary between the Carolina and the Brunswick (Charleston) terranes (Higgins & Zietz, 1983; Williams & Hatcher, 1982) and the revised location of an Alleghanian suture zone of Boote and Knapp (2016) (Figures 2b and 3a). The boundary between the Mid-Atlantic and New England Regions coincides with the Delaware Bay Fracture Zone in the Atlantic JQZ (Klitgord & Schouten, 1986) before bending northward in the IMQZ to maintain a strike perpendicular to IMA1–IMA5, where it aligns with a lateral offset of IMA1–IMA5 documented in this study and intersects a major gap between ECMA segments offshore Delaware (Figures 2b and 3a). The northern boundary of the New England Region is the New England Seamount Chain, which may have formed along a fracture zone, and also intersects a major gap between ECMA segments offshore Massachusetts (Figures 2b and 3a) (de Boer et al., 1988). Based on our observed association of our newly interpreted offsets of IMA1–IMA5 and the boundaries between the three Atlantic JQZ regions of distinct magnetic anomaly character with (i) evidence of rifting segmentation (e.g., Behn & Lin, 2000) and (ii) in some cases, hypothesized sutures at terrane boundaries (e.g., Boote & Knapp, 2016; Higgins & Zietz, 1983; Sawyer, 1985; Williams & Hatcher, 1982) (Figures 2b and 3a), we suggest that the preexisting margin structure and rifting segmentation of the ENAM have influenced the subsequent seafloor spreading regimes in the Atlantic JQZ.

### 5.4. Early ENAM Formation History From the ECMA to M25

Using our new Atlantic JQZ magnetic anomaly interpretations, we propose a crustal formation and evolution model from the ECMA to M25, specifically highlighting a missing piece of the ENAM history and early Atlantic opening (Figures 1a and 8a–8g). The IMQZ, bounded to the west by the ECMA, is the oldest crust of the Atlantic JQZ and was possibly formed by igneous activity associated with early seafloor spreading or late synrift magmatism, producing IMA1–IMA5 (Figures 2b, 3b). If the IMQZ is composed of oceanic crust, we suggest the initial seafloor spreading of the Atlantic following continental rifting was perpendicular to the margin using the consistent IMA1–IMA5 strike parallel to the ECMA, along with the IMA1–IMA5 offsets possibly representing fracture zones oriented approximately perpendicular to the ECMA, as indicators of seafloor spreading direction (Figures 2b and 3). However, the lack of magnetic anomaly ages/chron numbers for IMA1–5 causes difficulty in determining a preferred scenario for the early Atlantic formation. A ridge jump at the BSMA (Bird et al., 2007; Klitgord & Schouten, 1986; Kneller et al., 2012; Schettino & Turco, 2009; Vogt, 1973; Vogt, 1986) would produce IMA1/IMA5 and IMA2/IMA4 as conjugate magnetic anomalies, with IMA3 in the center as the youngest, while a drastic change in spreading rate and direction at the BSMA (Labails et al., 2010) would produce independent magnetic anomalies younging from IMA5 to IMA1 (Figures 2b and 3b). Likewise, if IMA1–IMA5 are the result of synrift magmatism, we suggest that rifting occurred approximately perpendicular to the margin during the formation of the IMQZ, with igneous emplacement occurring along the rift axis similar to observations along the nascent seafloor spreading near the Afar Depression (e.g., Bridges et al., 2012).

Following the formation of the IMQZ, the crust producing the BSMA was created (Figures 2 and 8b), which has been proposed to be related to either a ridge jump or a spreading rate/direction change (Bird et al., 2007; Klitgord & Schouten, 1986; Kneller et al., 2012; Labails et al., 2010; Schettino & Turco, 2009; Vogt, 1973). In this study, we are unable to determine whether the source of the BSMA is oceanic crust produced by seafloor spreading (e.g., Labails et al., 2010) or a sliver of continental crust and igneous intrusives isolated from the African margin by a ridge jump (e.g., Vogt, 1973). Nevertheless, if the BSMA source is crust emplaced by seafloor spreading (regardless of if a ridge jump occurred or not), the similarity in magnetic anomaly character between the BSMA and M42 in our synthetic profiles (see Profile 1 in Figure 4) could indicate that the BSMA may be M42, suggesting an age of ~168.5 Ma that is consistent with the BSMA ages of previous studies

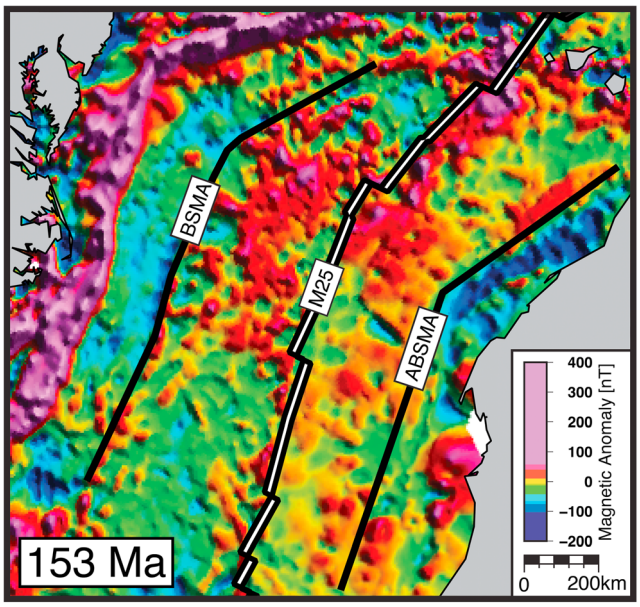


**Figure 9.** Plate reconstruction at 153 Ma, just following the creation of M25, the oldest generally accepted chron in the Atlantic, at ~155 Ma showing the ENAM and northwestern African margin and the EMAG2v3 composite magnetic anomaly grid (Meyer et al., 2016). Compares the orientation of the BSMA/Atlantic Blake Spur Magnetic Anomaly (ABSMA) orientation and the paleo-Mid-Atlantic Ridge at M25. Note that south of the bend in the BSMA/ABSMA, the BSMA/ABSMA are oriented parallel to M25, while to the north, the BSMA and ABSMA parallel each other but are oblique to M25. ABSMA interpretation is based on Labails et al. (2010).

(168–171 Ma) (Benson, 2003; Klitgord & Schouten, 1986). Alternatively, if the BSMA is produced by an isolated sliver of continental crust and igneous intrusives (e.g., Vogt, 1973), the similarity of the magnetic anomaly character between the BSMA and M42 is merely coincidental, as the BSMA would not be sourced to crust produced by seafloor spreading.

Continuing after the formation of the BSMA, the OMQZ formed (Figures 2 and 8c–8g). Our magnetic anomaly correlations in the New England, Mid-Atlantic, and Carolina Regions, along with anomalous ellipsoidal magnetic features such as the HFMAH, show that the seafloor spreading history from the BSMA to M25 was dictated by asymmetric crustal accretion and ridge orientations, possibly accompanied by short lived propagating rifts. Across the New England Region, the strike of magnetic anomaly lineations rotate counterclockwise from ~70° to ~55° (west to east) between the BSMA and M25 (Figures 2b and 8b–8g), and the calculated seafloor spreading rates are slower in the northern part of the New England Region compared to those further south (~12 mm/yr on Profiles 6 and 7 versus ~20 mm/yr on Profiles 1, 2, and 4). The change in magnetic anomaly strike in the New England Region indicates a change in ridge orientation during the formation of the OMQZ.

The conjugate Northwest African Margin shows a similar change in magnetic anomaly orientation between the African Blake Spur Magnetic Anomaly (ABSMA), a possible conjugate to the BSMA (Labails et al., 2010), and M25. A plate reconstruction to 153 Ma, using the GPlates software package (Boyden et al., 2011) and the rotation poles from the recent global plate reconstruction model of Müller et al. (2016), shows that the ABSMA has a strike mirroring that of the BSMA (Figure 9) (Labails et al., 2010). For the Mid-Atlantic and Carolina Regions and their conjugates, the BSMA/ABSMA are oriented parallel to M25, while for the New England Region and its conjugate, the BSMA and ABSMA parallel each other but are oblique to M25 (Figure 9). Additionally, the distance between the BSMA and M25 becomes narrower moving northward in the New England Region, while the corresponding distance between the ABSMA and M25 on the Northwestern African Margin becomes wider moving northward (Figure 9). Regardless if the ABMSA is the conjugate to the BSMA or not (e.g., Klitgord & Schouten, 1986; Labails et al., 2010; Schettino & Turco, 2009), the orientation of these linear magnetic anomalies on the either side of the Atlantic is consistent.

### 5.5. Crustal Accretion Style During the Early Formation of the ENAM

To account for both the slower spreading rates and magnetic anomaly lineation strike change in the New England Region (and its conjugate on the Northwest African margin), we suggest asymmetric crustal accretion occurred during the formation of the OMQZ crust of the western North Atlantic, causing a reorientation of the ridge during the formation of the OMQZ from the bend of the ECMA, IMA1–IMA5, and BSMA to the more linear strike of the M25 lineations and contemporaneous Mid-Atlantic Ridge (Figures 8 and 9). Spreading center reorientations have globally been identified based on rotations of magnetic anomaly lineation trends, caused by the asymmetric accretion of crust on either side of a spreading center. Ramberg et al., (1977) documented a spreading axis reorientation of the Mid-Atlantic Ridge southwest of the Azores, which they propose was facilitated by a combination of asymmetric spreading and small (5–10 km) ridge jumps of individual ridge segments. Likewise, Rona and Gray (1980) identified reorientations of the Mid-Atlantic Ridge in the young seafloor between the Kane and Atlantis Fracture Zones, which they attribute to asymmetric seafloor spreading. At the Juan de Fuca Ridge, Menard and Atwater (1968) and Wilson et al. (1984) suggest that the ridge reorientation could be facilitated by either asymmetric spreading or ridge jumps (with which they find associated propagating rifts), respectively. Altogether, asymmetric crustal accretion mechanisms could account for the ridge reorientation observed between the BSMA/ABSMA and M25 (Figures 8b–8g), with the asymmetric accretion caused by (1) asymmetric seafloor spreading, with slower spreading in

the northern New England Region on the North American side and faster spreading on the African side (Figure 8h) and/or (2) small, successive westward ridge jumps during the formation of the New England Region that adjusted the orientation of the ridge (Figure 8i). With either mechanism (or a combination of both), the change in orientation observed on the Northwest African Margin and asymmetric crustal accretion balances that on the ENAM in the New England Region (Figure 9).

We do not directly interpret any missing chrons indicative of ridge jumps in the New England region, but the presence of ridge jumps could not entirely be omitted as a mechanism responsible for the reorientation since ridge jumps could have occurred between the identified chrons in the OMQZ (Figure 2b). Additionally, if ridge jumps occurred, the entirety of the ridge in the New England Region did not necessarily jump simultaneously; rather, individual spreading segments may have jumped independently, with the combined overall effect of changing the ridge orientation (e.g., Ramberg et al., 1977). Either mechanism of asymmetric accretion or a combination of both would create the comparatively lower seafloor spreading rates calculated in the New England Region while changing the ridge orientation (Figures 8b–8g). If asymmetric seafloor spreading occurred, a slower spreading on the North American side of the ridge in the New England Region would produce the lower rates (Figure 8h). If westward ridge jumps occurred in the New England Region, the crust formed on the North American side of the ridge would be transferred to the African side, causing an apparently slower spreading rate due to the reduced amount of seafloor remaining (Figure 8i).

Changes in plate motion are a potential cause of asymmetric accretion and changes in spreading axis orientations (e.g., Menard & Atwater, 1968; Wilson et al., 1984). At the ENAM, Labails et al. (2010) suggested a change in plate motion, from NNW–SSE to NW–SE, occurred at the BSMA. If this change in plate motion occurred, coinciding with the beginning of the OMQZ formation (Figure 8b), it may have triggered the spreading axis reorientation observed in the New England Region (Figures 8c–8g), as the BSMA in this region is oriented more oblique to the new spreading direction compared to the BSMA of the Mid-Atlantic/Carolina Regions and M25 (Figures 8b–8g and 9).

Short-lived propagating rift segments, such as those hypothesized to be represented by the HFMAH, could have further contributed to the change in spreading center orientation (Figures 2 and 8a–2g). We suggest that these propagating rifts lined up seaward of the bend observed in the ECMA and the coastline at the New York Bight, near the boundary between the Mid-Atlantic and New England Regions, where it may have helped accommodate the spreading center straightening to that observed at M25 (Figures 8c and 8d), as propagating rifts have been found to be accompanied by changes in spreading center strike (Hey et al., 1980, 1988, 1986).

South of the New England Region, in the Mid-Atlantic and Carolina Regions, the identified magnetic anomaly lineations are all approximately parallel to both the BSMA and M25, and the calculated spreading rates are consistent (~20 mm/yr) (Figures 2b and 8b–8g and Table 2). This suggests that the seafloor spreading forming the OMQZ in the Mid-Atlantic and Carolina Regions proceeded without any ridge reorientation (Figures 8b–8g). Overall, seafloor spreading from M25 to the present-day Mid-Atlantic Ridge has taken place without the notable along strike variation in spreading rates and spreading axis reorientation observed in the OMQZ (Figures 2b, 5, and 8g and Table 2) (Bird et al., 2007; Klitgord & Schouten, 1986; Labails et al., 2010; Müller et al., 2008; Schettino & Turco, 2009; Tominaga & Sager, 2010a, 2010b).

## 6. Conclusions

From this study we draw the following conclusions:

1. Five newly identified coherent, correlatable magnetic anomalies exist along the entire margin in the IMQZ, which could be related to the earliest seafloor spreading of the Atlantic or igneous emplacement during the final stages of continental rifting.
2. If the source of the BSMA is oceanic crust, the BSMA may be M series anomaly M42 (~168.5 Ma) based on the similarity of magnetic anomaly character between the BSMA and M42.
3. Seafloor spreading rates during the formation of the OMQZ in the northwestern Atlantic were slower in the north compared to the south, and a 15° counterclockwise reorientation of the spreading axis occurred and straightened the prominent bend in the ECMA to the more linear strike of M25 and the contemporaneous Mid-Atlantic Ridge, possibly caused by asymmetric spreading and/or westward ridge jumps.

4. The HFMAH may be sourced from magma emplaced during a short-lived propagating rift that may have helped accommodate the straightening of the ridge during the formation of the OMQZ.
5. The newly identified magnetic anomalies and lineations offsets documented in this study possibly refine fracture zone locations in the IMQZ and OMQZ. These interpreted offsets that could indicate fracture zones project into segmentation in ECMA, which may support earlier hypotheses that preexisting margin structure controlled rift segments, which in turn influenced segmentation in the ECMA and the subsequent seafloor spreading regimes in the Atlantic JQZ.

**Acknowledgments**
The authors thank the captain and crew of the R/V *Langseth* MGL1407, MGL1408, and MGL1506 and R/V *Neil Armstrong* AR1-06 cruises. J. A. G. and M. T. thank the Department of Geology and Geophysics at Texas A&M University for their support of J. A. G.'s PhD program. M. T. and M. R. K. thank the Department of Earth and Environmental Sciences at Michigan State University for their support during M. R. K.'s MS thesis project, included in this study. We appreciate the constructive comments and suggestions from David Foster and two anonymous reviewers. Thank you to Matthew Arsenault for monitoring the at-sea acquisition for data quality. The opinions, findings, and conclusions stated herein are those of the authors and do not necessarily reflect those of the U.S. Extended Continental Shelf (ECS) Project. Any use of trade, firm, or product names is for descriptive purposes only and does not imply endorsement by the U.S. Government. Data for this work were provided by the U.S. ECS Project (Arsenault et al., 2017) and the GeoPRISMS ENAM Community Seismic Experiment (www.geoprisms.org). Archived data acquired from the National Centers for Environmental Information (www.ncei.noaa.gov). The comprehensive, georeferenced data set used in this study can be obtained in the supporting information (Data Set S1).

## References

Amante, C., & Eakins, B. W. (2009). *ETOPO1 1 arc-minute global relief model: Procedures, data sources and analysis, NOAA technical memorandum NESDIS NGDC-24* (pp. 1–19). Boulder, CO: National Geophysical Data Center, Marine Geology and Geophysics Division. https://doi.org/10.7289/V5C8276M

Andrews, B. D., Chaytor, J. D., ten Brink, U. S., Brothers, D. S., Gardner, J. V., Lobecker, E. A., & Calder, B. R. (2016). Bathymetric terrain model of the Atlantic margin for marine geological investigations (ver. 2.0, May 2016): U.S. Geological Survey open-file report 2012–1266, 19 p., 1 pl. https://doi.org/10.3133/ofr20121266

Arsenault, M. A., Miller, N. C., Hutchinson, D. G., Baldwin, W. E., Moore, E. M., Foster, D. F., … Fortin, W. F. (2017). Geophysical data collected along the Atlantic continental slope and rise 2014, U.S. Geological Survey Field Activity 2014-011-FA, cruise MGL1407: U.S. Geological Survey data release. https://doi.org/10.5066/F7V69HHS

Austin, J. A., Stoffa, P. L., Phillips, J. D., Oh, J., Sawyer, D. S., Purdy, G. M., … Makris, J. (1990). Crustal structure of the Southeast Georgia embayment-Carolina Trough: Preliminary results of a composite seismic image of a continental suture (?) and a volcanic passive margin. *Geology*, *18*(10), 1023–1027. http://10.0.4.106/0091-7613(1990)018%3C1023:CSOTSG%3E2.3.CO;2

Bankey, V., Cuevas, A., Daniels, D., Finn, C. A., Hernandez, I., Hill, P., … Ravat, D. (2002). Digital data grids for the magnetic anomaly map of North America. U.S. Geological Survey Open-File Report 02-414.

Barrett, D. L., & Keen, C. E. (1976). Mesozoic magnetic lineations, the magnetic quiet zone, and sea floor spreading in the northwest Atlantic. *Journal of Geophysical Research*, *81*(26), 4875–4884. https://doi.org/10.1029/JB081i026p04875

Bazin, S., Harding, A., Kent, G., Orcutt, J., Tong, C., Pye, J., … White, R. (2001). Three-dimensional shallow crustal emplacement at the 9°03′N over-lapping spreading center on the East Pacific Rise: Correlations between magnetization and tomographic images. *Journal of Geophysical Research*, *106*(B8), 16,101–16,117. https://doi.org/10.1029/2001JB000371

Behn, M. D., & Lin, J. (2000). Segmentation in gravity and magnetic anomalies along the U.S. East Coast passive margin: Implications for incipient structure of the oceanic lithosphere. *Journal of Geophysical Research*, *105*(B11), 25,769–25,790. https://doi.org/10.1029/2000JB900292

Benson, R. N. (2003). Age estimates of the seaward-dipping volcanic wedge, earliest oceanic crust, and earliest drift-stage sediments along the North American Atlantic continental margin. *Geophysical Monograph Series*, *136*, 61–75. https://doi.org/10.1029/136GM04

Biari, Y., Klingelhoefer, F., Sahabi, M., Funck, T., Benabdellouahed, M., Schnabel, M., … Austin, J. A. (2017). Opening of the central Atlantic Ocean: Implications for geometric rifting and asymmetric initial seafloor spreading after continental breakup. *Tectonics*, *36*(6), 1129–1150. https://doi.org/10.1002/2017TC004596

Bird, D. E., Hall, S. A., Burke, K., Casey, J. F., & Sawyer, D. S. (2007). Early Central Atlantic Ocean seafloor spreading history. *Geosphere*, *3*(5), 282–298. https://doi.org/10.1130/GES00047.1

Boote, S. K., & Knapp, J. H. (2016). Offshore extent of Gondwanan Paleozoic strata in the southeastern United States : The Suwannee suture zone revisited. *Gondwana Research*, *40*, 199–210. https://doi.org/10.1016/j.gr.2016.08.011

Boyden, J. A., Müller, R. D., Gurnis, M., Torsvik, T. H., Clark, J. A., Turner, M., … Cannon, J. S. (2011). Nest-generation plate-tectonic reconstructions using GPlates. In G. R. Keller & C. Baru (Eds.), *Geoinformatics: Cyberinfrastructure for the Solid Earth Sciences* (pp. 95–114). Cambridge, UK: Cambridge University Press. https://doi.org/10.1017/CBO9780511976308.008

Bridges, D. L., Mickus, K., Gao, S. S., Abdelsalam, M. G., & Alemu, A. (2012). Magnetic stripes of a transitional continental rift in afar. *Geology*, *40*(3), 203–206. https://doi.org/10.1130/G32697.1

Bronner, A., Sauter, D., Manatschal, G., Péron-Pinvidic, G., & Munschy, M. (2011). Magmatic breakup as an explanation for magmatic anomalies at magma-poor rifted margins. *Nature Geoscience*, *4*(8), 549–553. https://doi.org/10.1038/NGEO1201

Butman, B., Twichell, D. C., Rona, P. A., Tucholke, B. E., Middleton, T. J., & Robb, J. M. (2006). Seafloor topography and backscatter intensity of the Hudson Canyon Region Offshore of New York and New Jersey. U.S. Geological Survey Open-File Report 2004–1411.

Chapman, M. C., & Beale, J. N. (2010). On the geologic structure at the epicenter of the 1886 Charleston, South Carolina, earthquake. *Bulletin of the Seismological Society of America*, *100*(3), 1010–1030. https://doi.org/10.1785/0120090231

Chaytor, J. D., Twichell, D. C., ten Brink, U. S., Buczkowski, B. J., & Andrews, B. D. (2007). Revisiting submarine mass movements along the U.S. Atlantic continental margin: Implications for tsunami hazards. In V. Lykousis, D. Sakellariou, & J. Locat (Eds.), *Submarine mass movements and their consequences* (pp. 395–403). Switzerland: Springer. https://doi.org/10.1007/978-1-4020-6512-5_41

de Boer, J. Z., McHone, G., Puffer, J. H., Ragland, P. C., & Whillington, D. (1988). Mesozoic and Cenozoic magmatism. In R. E. Sheridan & J. A. Grow (Eds.), *The Geology of North America, I-2, the Atlantic continental margin, U.S.* (pp. 217–241). Boulder, CO: Geological Society of America.

Dillon, W. P., Manheim, F. T., Jansa, L. F., Pálmason, G., Tucholke, B. E., & Landrum, R. S. (1986). Resource potential of the western North Atlantic Basin. In P. R. Vogt & B. E. Tucholke (Eds.), *The geology of North America, Vol. M, the Western North Atlantic Region*, (pp. 661–676). Boulder, CO: Geological Society of America.

Dunbar, J. A., & Sawyer, D. S. (1989). How preexisting weaknesses control the style of continental breakup. *Journal of Geophysical Research*, *94*(B6), 7278. https://doi.org/10.1029/JB094iB06p07278

Duncan, R. A. (1984). Age progressive volcanism in the New England seamounts and the opening of the central Atlantic Ocean. *Journal of Geophysical Research*, *89*(B12), 9980–9990. https://doi.org/10.1029/JB089iB12p09980

Embley, R. M., & Jacobi, R. (1986). Mass wasting in the western North Atlantic. In P. R. Vogt & B. E. Tucholke (Eds.), *The geology of North America, Vol. M, the Western North Atlantic Region* (pp. 479–490). Boulder, CO: Geological Society of America.

Finlay, C. C., Maus, S., Beggan, C. D., Bondar, T. N., Chambodut, A., Chernova, T. A., … Zvereva, T. I. (2010). International geomagnetic reference field: The eleventh generation. *Geophysical Journal International*, *183*(3), 1216–1230.

Folger, D. W. (1988). Geologic hazards of the Atlantic continental margin. In R. E. Sheridan & J. A. Grow (Eds.), *The geology of North America, Vol. I-2, the Atlantic Continental Margin: U.S* (pp. 529–548). Boulder, CO: Geological Society of America.

Gardner, W. D. (1989). Baltimore canyon as a modern conduit of sediment to the deep sea. *Deep Sea Research Part A: Oceanographic Research Papers*, *36*(3), 323–358. https://doi.org/10.1016/0198-0149(89)90041-1

Grauch, V. J. S., Hudson, M. R., Minor, S. A., & Caine, J. S. (2006). Sources of along-strike variation in magnetic anomalies related to intrasedimentary faults: A case study from the Rio Grande Rift, USA. *Exploration Geophysics*, *37*(4), 372–378. https://doi.org/10.1071/EG06372

Grow, J. A., Klitgord, K. D., & Schlee, J. S. (1988). Structure and evolution of Baltimore Canyon Trough. In R. E. Sheridan & J. A. Grow (Eds.), *The geology of North America, Vol. I-2, the Atlantic Continental Margin: U.S* (pp. 269–290). Boulder, CO: Geological Society of America.

Gudmundsson, A. (1993). On the structure and formation of fracture-zones. *Terra Nova*, *5*(3), 215–224. https://doi.org/10.1111/j.1365-3121.1993.tb00252.x

Gunn, P. J. (1997). Regional magnetic and gravity responses of extensional sedimentary basins. *Journal of Australian Geology and Geophysics*, *17*(2), 115–131.

Hatcher, R. D. (1989). Tectonic synthesis of the U.S. Appalachians. In R. D. Hatcher, W. A. Thomas, & G. W. Viele (Eds.), *The Geology of North America, Vol. F-2, the Appalachian-Ouachita Orogen in the United States* (pp. 511–535). Boulder, CO: Geological Society of America.

Hatcher, R. D. (2010). The Appalachian orogen: A brief summary. *Geological Society of America Memoirs*, *206*(1), 1–19. https://doi.org/10.1130/2010.1206(01)

Hey, R. N. (1977). A new class of "pseudofaults" and their bearing on plate tectonics: A propagating rift model. *Earth and Planetary Science Letters*, *37*(2), 321–325. https://doi.org/10.1016/0012-821X(77)90177-7

Hey, R. N., Duennebier, F. K., & Morgan, W. J. (1980). Propagating rifts on mid-ocean ridges. *Journal of Geophysical Research*, *85*(B7), 3647–3658. https://doi.org/10.1029/JB085iB07p03647

Hey, R. N., Kleinrock, M. C., Miller, S. P., Atwater, T. M., & Searle, R. C. (1986). Sea Beam/Deep-Tow Investigation of an Active Oceanic Propagating Rift System, Galapagos 95.5°W. *Journal of Geophysical Research*, *91*(B3), 3369–3393.

Hey, R. N., Menard, H. W., Atwater, T. M., & Caress, D. W. (1988). Changes in direction of seafloor spreading revisited. *Journal of Geophysical Research*, *93*(B4), 2803–2811. https://doi.org/10.1029/JB093iB04p02803

Hey, R. N., & Wilson, D. S. (1982). Propagating rift explanation for the tectonic evolution of the northeast Pacific the pseudomovie. *Earth and Planetary Science Letters*, *58*(2), 167–184. https://doi.org/10.1016/0012-821X(82)90192-3

Higgins, M. W., & Zietz, I. (1983). Geological interpretation of geophysical maps of the pre-Cretaceous "basement" beneath the coastal plain of the southeaster Unites States. *Geological Society of America Memoirs*, *158*, 125–130. https://doi.org/10.1130/MEM158-p125

Hollister, C. D., Ewing, J. I., Habib, D., Hathaway, J. C., Lancelot, Y., Luterbacher, H., … Worstell, P. (1972). *Initial reports of the Deep Sea Drilling Project* (Vol. 11, pp. 313–349). Washington, DC: U.S. Government Printing Office.

Horen, H., & Fleutelot, C. (1998). Highly magnetized and differentiated basalts at the 18–19° S propagating spreading center in the North Fiji Basin. *Marine Geophysical Researches*, *20*(2), 129–137. https://doi.org/10.1023/A:1004457812905

Horton, J. W. Jr., Drake, A. A. Jr., & Rankin, D. R. (1989). Tectonostratigraphic terranes and their Paleozoic boundaries in the central and southern Appalachians. *Geological Society Special Papers*, *230*, 213–246. https://doi.org/10.1130/SPE230-p213

Johnson, P., & Pariso, J. E. (1993). Do layer 3 rocks make a significant contribution to marine magnetic anomalies? In situ magnetization of gabbros at Ocean Drilling Program hole 735B. *Journal of Geophysical Research*, *98*(B1), 435–445. https://doi.org/10.1029/93JB01097

Keen, C. E., & Potter, D. P. (1995a). The transition from a volcanic to a nonvolcanic rifted margin off eastern Canada. *Tectonics*, *14*(2), 359–371. https://doi.org/10.1029/94TC03090

Keen, C. E., & Potter, D. P. (1995b). Formation and evolution of the Nova Scotian rifted margin: Evidence from deep seismic reflection data. *Tectonics*, *14*(4), 918–932. https://doi.org/10.1029/95TC00838

Kelemen, P. B., & Holbrook, W. S. (1995). Origin of thick, high-velocity igneous crust along the U.S. East Coast Margin. *Journal of Geophysical Research*, *100*(B6), 10,077–10,094. https://doi.org/10.1029/95JB00924

Keller, F. Jr., Meuschke, J. L., & Alldredge, L. R. (1954). Aeromagnetic surveys in the Aleutian, Marshall, and Bermuda Islands. *Eos, Transactions American Geophysical Union*, *35*(4), 558–572. https://doi.org/10.1029/TR035i004p00558

Klitgord, K. D., & Behrendt, J. C. (1977). Aeromagnetic map of the United States Atlantic continental margin: U.S. Geological Survey Miscellaneous Field Studies Map MF-913, 2 sheets, scale 1:1,000,000.

Klitgord, K. D., & Grow, J. A. (1980). Jurassic seismic stratigraphy and basement structure of western Atlantic magnetic quiet zone. *AAPG Bulletin*, *64*(10), 1658–1680.

Klitgord, K. D., & Schouten, H. (1986). Plate kinematics of the central Atlantic. In P. R. Vogt & B. E. Tucholke (Eds.), *The Geology of North America, Vol. M, the Western North Atlantic Region* (pp. 351–378). Boulder, CO: Geological Society of America.

Klitgord, K. D., Hutchinson, D. R., & Schouten, H. (1988). U.S. Atlantic continental margin; structural and tectonic framework. In R. E. Sheridan & J. A. Grow (Eds.), *The Geology of North America, I-2, the Atlantic Continental Margin, U.S* (pp. 19–56). Boulder, CO: Geological Society of America.

Kneller, E. A., Johnson, C. A., Karner, G. D., Einhorn, J., & Queffelec, T. A. (2012). Inverse methods for modeling non-rigid plate kinematics: Application to mesozoic plate reconstructions of the Central Atlantic. *Computers & Geosciences*, *49*, 217–230. https://doi.org/10.1016/j.cageo.2012.06.019

Labails, C., Olivet, J. L., Aslanian, D., & Roest, W. R. (2010). An alternative early opening scenario for the Central Atlantic Ocean. *Earth and Planetary Science Letters*, *297*(3-4), 355–368. https://doi.org/10.1016/j.epsl.2010.06.024

Larson, R. L., & Pitman, W. C. (1972). World-wide correlation of Mesozoic magnetic anomalies and its implications. *Geological Society of America Bulletin*, *83*(12), 3645–3662. https://doi.org/10.0.4.106/0016-7606(1972)83[3645:WCOMMA]2.0.CO;2

Lizarralde, D., & Holbrook, W. S. (1997). U.S. Mid-Atlantic margin structure and early thermal evolution. *Journal of Geophysical Research*, *102*(B10), 22,855–22,875. https://doi.org/10.1029/96JB03805

Lowrie, A. Jr., & Heezen, B. C. (1967). Knoll and sediment drift near Hudson Canyon. *Science*, *157*, 1152–1153.

Manspeizer, W. (1988). Triassic-Jurassic rifting and the opening of the Atlantic: An overview. In W. Manspeizer (Ed.), *Triassic-Jurassic Rifting* (pp. 41–79). Amsterdam: Elsevier.

Marzoli, A., Renne, P. R., Piccirillo, E. M. E. M., Ernesto, M., Bellieni, G., & De Min, A. (1999). Extensive 200-million-year-old continental flood basalts of the Central Atlantic Magmatic Province. *Science*, *284*(5414), 616–618. https://doi.org/10.1126/science.284.5414.616

Mattick, R. E., & Libby-French, J. (1986). Petroleum geology of the United States Atlantic continental margin. In P. R. Vogt & B. E. Tucholke (Eds.), *The geology of North America, Vol. M, the Western North Atlantic Region* (pp. 445–462). Boulder, CO: Geological Society of America.

McBride, J. H., & Nelson, K. D. (1988). Integration of COCORP-deep reflection and magnetic anomaly analysis in the southeastern United States: Implications for origin of the Brunswick and East Coast magnetic anomalies. *Geological Society of America Bulletin*, *100*(3), 436–445. https://doi.org/10.0.4.106/0016-7606(1988)100%3C0436:IOCDRA%3E2.3.CO;2

Mchone, J. G. (2000). Non-plume magmatism and rifting during the opening of the central Atlantic Ocean. *Tectonophysics*, *316*(3-4), 287–296. https://doi.org/10.1016/S0040-1951(99)00260-7

Menard, H. W., & Atwater, T. (1968). Changes in direction of sea floor spreading. *Nature*, *219*(5153), 463–467. https://doi.org/10.1038/219463a0

Meyer, B., Saltus, R., & Chulliat, A. (2016). EMAG2: Earth magnetic anomaly grid (2-arc-minute resolution) version 3. National Centers for Environmental Information, NOAA. Model. https://doi.org/10.7289/V5H70CVX

Miller, S. P., & Hey, R. N. (1986). Three-dimensional magnetic modeling of a propagating rift, Galapagos 95°30′W. *Journal of Geophysical Research*, *91*(B3), 3395–3406. https://doi.org/10.1029/JB091iB03p03395

Müller, R. D., & Roest, W. R. (1992). Fracture zones in the North Atlantic from combined Geosat and Seasat data. *Journal of Geophysical Research*, *97*(B3), 3337–3350. https://doi.org/10.1029/91JB02605

Müller, R. D., Roest, W. R., Royer, J. Y., & Sclater, J. G. (1997). Digital isochrons of the world's ocean floor. *Journal of Geophysical Research*, *102*(B2), 3211–3214. https://doi.org/10.1029/96JB01781

Müller, R. D., Sdrolias, M., Gaina, C., & Roest, W. R. (2008). Age, spreading rates, and spreading asymmetry of the world's ocean crust. *Geochemisty, Geophysics, Geosystems*, *9*(4), 1–19. https://doi.org/10.1029/2007GC001743

Müller, R. D., Seton, M., Zahirovic, S., Williams, S. E., Matthews, K. J., Wright, N. M., … Cannon, J. (2016). Ocean basin evolution and global-scale plate reorganization events since Pangea breakup. *Annual Review of Earth and Planetary Sciences*, *44*(1), 107–138. https://doi.org/10.1146/annurev-earth-060115-012211

Nomade, S., Knight, K. B., Beutel, E., Renne, P. R., Verati, C., & Féraud, G. (2007). Chronology of the Central Atlantic Magmatic Province: Implications for the Central Atlantic rifting processes and the Triassic – Jurassic biotic crisis. *Palaeogeography Palaeoclimatology Palaeoecology*, *244*(1-4), 326–344. https://doi.org/10.1016/j.palaeo.2006.06.034

Ogg, J. G. (2012). Geomagnetic polarity time scale. In F. M. Gradstein et al. (Eds.), *The geologic time scale* (pp. 85–113). Amsterdam: Elsevier. https://doi.org/10.1016/B978-0-444-59425-9.00005-6

Oh, J., Austin, J. A., Phillips, J. D., Coffin, M. F., & Stoffa, P. L. (1995). Seaward-dipping reflectors offshore the southeastern United States: Seismic evidence for extensive volcanism accompanying sequential formation of the Carolina Trough and Blake Plateau Basin. *Geology*, *23*(1), 9–12. https://doi.org/10.0.4.106/0091-7613(1995)023%3C0009:SDROTS%3E2.3.CO;2

Olsen, P. E., Kent, D. V., Et-Touhami, M., & Puffer, J. H. (2003). Cyclo-, magneto-, and bio-stratigraphy constraints on the duration of the CAMP event and its relationship to the Triassic-Jurassic boundary. In *The Central Atlantic Magmatic Province: Insights from Fragments of Pangea*, *Geophysical Monograph Series* (Vol. 136, pp. 7–32). https://doi.org/10.1029/136GM02

Oufi, O., & Cannat, M. (2002). Magnetic properties of variably serpentinized abyssal peridotites. *Journal of Geophysical Research*, *107*(B5), 2095. https://doi.org/10.1029/2001JB000549

Parker, R. L. (1973). The rapid calculation of potential anomalies. *Geophysical Journal International*, *31*(4), 447–455. https://doi.org/10.1111/j.1365-246X.1973.tb06513.x

Pilkey, O. H., & Cleary, W. J. (1986). Turbidite sedimentation in the northwestern Atlantic Ocean basin. In P. R. Vogt & B. E. Tucholke (Eds.), *The Geology of North America, Vol. M, the Western North Atlantic Region* (pp. 437–450). Boulder, CO: Geological Society of America.

Poag, C. W., & Sevon, W. D. (1989). A record of Appalachian denundation in postrift Mesozoic and Cenozoic sedimentary deposits of the U.S. Middle Atlantic Continental Margin. *Geomorphology*, *2*(1-3), 119–157. https://doi.org/10.1016/0169-555X(89)90009-3

Poag, C. W., & Ward, L. W. (1993). Allostratigraphy of the U.S. middle Atlantic continental margin- characteristics, distribution, and depositional history of principle unconformity-bounded upper Cretaceous and Cenozoic sedimentary units, Geological Survey professional paper 1542, U.S. Geological Survey, Washington D.C.

QGIS Development Team (2015). QGIS geographic information system, Open Source Geospatial Foundation Project.

Ramberg, I. B., Gray, D. F., & Raynolds, R. G. H. (1977). Tectonic evolution of the FAMOUS area of the Mid-Atlantic Ridge, lat 35°50′ to 37°20′N. *Geological Society of America Bulletin*, *88*(5), 609–620. https://doi.org/10.0.4.106/0016-7606(1977)88%3C609:TEOTFA%3E2.0.CO;2

Riggs, S. R., & Manheim, F. T. (1988). Mineral resources of the U.S. Atlantic margin. In R. E. Sheridan & J. A. Grow (Eds.), *The geology of North America, I-2, the Atlantic Continental Margin, U.S* (pp. 501–520). Boulder, CO: Geological Society of America.

Roeser, H. A., Steiner, C., Schreckenberger, B., & Block, M. (2002). Structural development of the Jurassic Magnetic Quiet Zone off Morocco and identification of Middle Jurassic magnetic lineations. *Journal of Geophysical Research*, *107*(B10), 2207. https://doi.org/10.1029/2000JB000094

Roest, W. R., Danobeitia, J. J., Verhoef, J., & Collette, B. J. (1992). Magnetic-anomalies in the canary basin and the Mesozoic evolution of the central North-Atlantic. *Marine Geophysical Researches*, *14*(1), 1–24. https://doi.org/10.1007/Bf01674063

Rona, P. A., & Gray, D. F. (1980). Structural behavior of fracture zones symmetric and asymmetric about a spreading axis: Mid-Atlantic Ridge (latitude 23°N to 27°N). *Geological Society of America Bulletin*, *91*(8), 485–494. https://doi.org/10.0.4.106/0016-7606(1980)91%3C485:SBOFZS%3E2.0.CO;2

Rona, P. A., Brakl, J., & Heirtzler, J. R. (1970). Magnetic anomalies in the northeast Atlantic between the canary and Cape Verde Islands. *Journal of Geophysical Research*, *75*(35), 7412–7420. https://doi.org/10.1029/JB075i035p07412

Russell, S. M., & Whitmarsh, R. B. (2003). Magmatism at the west Iberia non-volcanic rifted continental margin: Evidence from analyses of magnetic anomalies. *Geophysical Journal International*, *154*(3), 706–730. https://doi.org/10.1046/j.1365-246X.2003.01999.x

Sahabi, M., Aslanian, D., & Olivet, J. L. (2004). A new starting point for the central Atlantic. *Comptes Rendus Geoscience*, *336*(12), 1041–1052. https://doi.org/10.1016/j.crte.2004.03.017

Sandwell, D. T., Müller, R. D., Smith, W. H. F., Garcia, E., & Francis, R. (2014). New global marine gravity model from CryoSat-2 and Jason-1 reveals buried tectonic structure. *Science*, *346*(6205), 65–67. https://doi.org/10.1016/j.crte.2004.03.017

Sawyer, D. S. (1985). Total tectonic subsidence: A parameter for distinguishing crust type at the U.S. Atlantic Continental Margin. *Journal of Geophysical Research*, *90*(B9), 7751–7769. https://doi.org/10.1029/JB090iB09p07751

Schettino, A. (2014). *Quantitative plate tectonics*. New York, NY: Springer.

Schettino, A., & Scotese, C. R. (2005). Apparent polar wander paths for the major continents (200 Ma to the present day): A paleomagnetic reference frame for global plate tectonic reconstructions. *Geophysical Journal International*, *163*(2), 727–759. https://doi.org/10.1111/j.1365-246X.2005.02638.x

Schettino, A., & Turco, E. (2009). Breakup of Pangaea and plate kinematics of the central Atlantic and atlas regions. *Geophysical Journal International*, *178*(2), 1078–1097. https://doi.org/10.1111/j.1365-246X.2009.04186.x

Schlische, R. W., Withjack, M. O., & Olsen, P. E. (2003). Relative timing of CAMP, rifting, continental breakup, and basin inversion: Tectonic significance. In W. E. Hames et al. (Eds.), *The Central Atlantic Magmatic Province: Insights from Fragments of Pangea*, *Geophysical Monograph Series* (Vol. 136, pp. 33–59). Washington, DC: American Geophysical Union. https://doi.org/10.1029/136GM03

Schouten, H., & Klitgord, K. D. (1977). Map showing Mesozoic magnetic anomalies: Western North Atlantic, U. S. Geol. Surv. Misc. Field Stud. Map, MF-195.
Schouten, H., & White, R. S. (1980). Zero-offset fracture zones. *Geology*, *8*, 175–179.
Sheridan, R. E. (1987). The passive margin of the U.S.A. *Episodes*, *10*(4), 254–258.
Sheridan, R. E. (1989). The Atlantic passive margin. In A. W. Bally & A. R. Palmer (Eds.), *The geology of North America: An overview, U.S* (pp. 81–96). Boulder, CO: Geological Society of America. https://doi.org/10.1130/DNAG-GNA-A.81
Sheridan, R. E., Musser, D. L., Glover, L., Talwani, M., Ewing, J. I., Holbrook, W. S., … Smithson, S. (1993). Deep seismic reflection data of EDGE U.S. mid-Atlantic continental- margin experiment: Implications for Appalachian sutures and Mesozoic rifting and magmatic underplating. *Geology*, *21*(6), 563–567. https://doi.org/10.0.4.106/0091-7613(1993)021%3C0563:DSRDOE%3E2.3.CO;2
Sinton, J. M., Wilson, D. S., Christie, D. M., Hey, R. L., & Delaney, J. R. (1983). Petrologic consequences of rift propagation on oceanic spreading ridges. *Earth and Planetary Science Letters*, *62*(2), 193–207. https://doi.org/10.1016/0012-821X(83)90083-3
Sundvik, M. T., & Larson, R. L. (1988). Seafloor spreading history of the western North Atlantic Basin derived from the Keathley sequence and computer graphics. *Tectonophysics*, *155*(1–4), 49–71. https://doi.org/10.1016/0040-1951(88)90260-0
Sweeney, E. M., Gardner, J. V., Johnson, J. E., & Mayer, L. A. (2012). Geological interpretation of a low-backscatter anomaly found on the New Jersey continental margin. *Marine Geology*, *326–328*, 46–54. https://doi.org/10.1016/j.margeo.2012.08.007
Talwani, M., & Abreu, V. (2000). Inferences regarding initiation of oceanic crust formation from the U.S. East Coast Margin and Conjugate South Atlantic Margins. *Geophysical Monograph Series*, *115*, 211–233.
Talwani, M., & Heirtzler, J. R. (1964). Computation of magnetic anomalies caused by two dimensional structures of arbitrary shape. In G. A. Parks (Ed.), *Computers in the mineral industry* (pp. 464–480). Stanford: Stanford University Press.
Talwani, M., Ewing, J., Sheridan, R. E., Holbrook, W. S., & Glover, L. III (1995). The EDGE experiment and the US East Coast magnetic anomaly. In E. Banda, M. Torné, & M. Talwani (Eds.), *Rifted ocean-continent boundaries* (pp. 155–181). Dordrecht, The Netherlands: Kluwer Academic. https://doi.org/10.1007/978-94-011-0043-4_9
Taylor, P. T., Zietz, I., & Dennis, L. S. (1968). Geologic implications of aeromagnetic data for the eastern continental margin of the United States. *Geophysics*, *33*(5), 775–780.
Tivey, M. A., Sager, W. W., Lee, S. M., & Tominaga, M. (2006). Origin of the Pacific Jurassic quiet zone. *Geological Society of America*, *34*(9), 789–792.
Tominaga, M., & Sager, W. W. (2010a). Origin of the smooth zone in early cretaceous North Atlantic magnetic anomalies. *Geophysical Research Letters*, *37*, L01304. https://doi.org/10.1029/2009GL040984
Tominaga, M., & Sager, W. W. (2010b). Revised Pacific M-anomaly geomagnetic polarity timescale. *Geophysical Journal International*, *182*, 203–232. https://doi.org/10.1111/j.1365-246X.2010.04619.x
Tominaga, M., Tivey, M. A., MacLeod, C. J., Lissenberg, C. J., Morris, A., Shillington, D. J., & Ferrini, V. (2016). Characterization of the in situ magnetic architecture of oceanic crust (Hess Deep) using near-source vector magnetic data. *Journal of Geophysical Research: Solid Earth*, *121*, 4130–4146. https://doi.org/10.1002/2015JB012783
Tréhu, A. M., Ballard, A., Dorman, L. M., Gettrust, J. F., Klitgord, K. D., & Schreiner, A. A. (1989). Structure of the lower crust beneath the Carolina Trough, U.S. Atlantic continental margin. *Journal of Geophysical Research*, *94*(B8), 10,585–10,600. https://doi.org/10.1029/JB094iB08p10585
Tucholke, B. E. (1986). Structure of the basement and distribution of sediments in the western North Atlantic Ocean. In P. R. Vogt & B. E. Tucholke (Eds.), *The geology of North America, Vol. M, the Western North Atlantic Region* (pp. 331–340). Boulder, CO: Geological Society of America.
Tucholke, B. E., & Schouten, H. (1988). Kane Fracture Zone. *Marine Geophysical Researches*, *10*(1-2), 1–39. https://doi.org/10.1007/BF02424659
Van Avendonk, H. J. A., Holbrook, W. S., Nunes, G. T., Shillington, D. J., Tucholke, B. E., Louden, K. E., … Hopper, J. R. (2006). Seismic velocity structure of the rifted margin of the eastern grand banks of Newfoundland, Canada. *Journal of Geophysical Research*, *111*, B11404. https://doi.org/10.1029/2005JB004156
Van Avendonk, H. J. A., Christeson, G. L., Norton, I. O., & Eddy, D. R. (2015). Continental rifting and sediment infill in the northwestern Gulf of Mexico. *Geology*, *43*(7), 631–634. https://doi.org/10.1130/G36798.1
Verhoef, J., Collette, B. J., Dañobeitia, J. J., Roeser, H. A., & Roest, W. R. (1990). Magnetic anomalies off West-Africa (20–38°N). *Marine Geophysical Researches*, *13*, 81–103.
Vogt, P. R. (1973). Early events in the opening of the North Atlantic. In D. H. Taling & S. K. Runcorn (Eds.), *Implications of continental rift to the Earth Sciences* (pp. 693–712). New York: Academic Press.
Vogt, P. R. (1986). Magnetic anomalies and crustal magnetization. In P. R. Vogt & B. E. Tucholke (Eds.), *The geology of North America, Vol. M, the Western North Atlantic Region* (pp. 229–256). Boulder, CO: Geological Society of America.
Vogt, P. R., Anderson, C. N., Bracey, D. R., & Schneider, E. D. (1970). North Atlantic magnetic smooth zones. *Journal of Geophysical Research*, *75*(20), 3955–3968. https://doi.org/10.1029/JB075i020p03955
Vogt, P. R., Anderson, C. N., & Bracey, D. R. (1971). Mesozoic magnetic anomalies, sea-floor spreading, and geomagnetic reversals in the southwestern North Atlantic. *Journal of Geophysical Research*, *76*(20), 4796–4823. https://doi.org/10.1029/JB076i020p04796
Wanless, V. D., Perfit, M. R., Klein, E. M., White, S., & Ridley, W. I. (2012). Reconciling geochemical and geophysical observations of magma supply and melt distribution at the 9°N overlapping spreading center, East Pacific Rise. *Geochemistry, Geophysics, Geosystems*, *13*(11), 1–22, Q11005.
Williams, H., & Hatcher, R. D. (1982). Suspect terranes and accretionary history of the Appalachian orogen. *Geology*, *10*(10), 530–536. https://doi.org/10.0.4.106/0091-7613(1982)10%3C530:STAAHO%3E2.0.CO;2
Wilson, J. T. (1966). Did the Atlantic close and then re-open? *Nature*, *211*(5050), 676–681. https://doi.org/10.1038/211676a0
Wilson, D. S., & Hey, R. N. (1995). History of rift propagation and magnetization for the Cocos-Nazca spreading center. *Journal of Geophysical Research*, *100*(B6), 10,041–10,056. https://doi.org/10.1029/95JB00762
Wilson, D. S., Hey, R. N., & Nishimura, C. (1984). Propagation as a mechanism of reorientation of the Juan de Fuca Ridge. *Journal of Geophysical Research*, *89*(B11), 9215–9225. https://doi.org/10.1029/JB089iB11p09215
Withjack, M. O., Schlische, R. W., & Olsen, P. E. (1998). Diachronous rifting, drifting, and inversion on the passive margin of central eastern North America: An analog for other passive margins. *AAPG Bulletin*, *82*(5A), 817–835.
Wyer, P., & Watts, A. B. (2006). Gravity anomalies and segmentation at the East Coast, USA continental margin. *Geophysical Journal International*, *166*(3), 1015–1038. https://doi.org/10.1111/j.1365-246X.2006.03066.x
Zietz, I. (1982). Composite magnetic anomaly map of the United States; Part A, Conterminous United States: U.S. Geological Survey Investigations Map GP-954-A, 59 pp., 2 sheets, scale 1:2,500,000.